



Published in final edited form as:

J Mater Chem B. 2020 April 21; 8(15): 2930–2950. doi:10.1039/d0tb00034e.

Materials and Technical Innovations in 3D Printing in Biomedical Applications

Hiroyuki Tetsuka^{a,b}, Su Ryon Shin^a

^aDivision of Engineering in Medicine, Department of Medicine, Brigham and Women's Hospital, Harvard Medical School, 65 Lansdowne Street, Cambridge, Massachusetts, 02139 USA

^bFuture Research Department, Toyota Research Institute of North America, Toyota Motor North America, 1555 Woodridge Avenue, Ann Arbor, Michigan, 48105 USA

Abstract

3D printing is a rapidly growing research area, which significantly contributes to major innovations in various fields of engineering, science, and medicine. Although the scientific advancement of 3D printing technologies has enabled the development of complex geometries, there is still an increasing demand for innovative 3D printing techniques and materials to address the challenges in building speed and accuracy, surface finish, stability, and functionality. In this review, we introduce and review the recent developments in novel materials and 3D printing techniques to address the needs of the conventional 3D printing methodologies especially in biomedical applications, such as printing speed, cell growth feasibility, and complex shape achievement. A comparative study of these materials and technologies with respect to the 3D printing parameters will be provided for selecting a suitable application-based 3D printing methodology. Discussion on prospects of 3D printing materials and technologies will be finally covered.

1. Introduction

Since the invention of the stereolithography (SLA) method and the creation of the first three-dimensional (3D) printed object during the 1980s by Hull,^{1, 2} 3D printing has been adopted in various areas such as engineering, manufacturing, medicine, and education, in a widespread way. Now, over the past 40 years, the technology has been evolving, bringing researchers the creation of the 3D objects with a complex geometry that was previously difficult using conventional fabrication techniques and an invention of the innovative systems.^{3–10} The progress in 3D printing enabled researchers to create complex objects, biomimetic tissue constructs, autonomous soft robots, and customized drug delivery systems, and facilitated the development of system designs with higher resolution and more precise control by combining the multi-material design, machine learning, and topological optimization algorithms.^{11–29}

sshin4@bwh.harvard.edu.

Conflicts of interest

There are no conflicts to declare.

Figure 1 summarizes the technical innovations and materials in the history of 3D printing. Conventional 3D printing processes, where 3D objects are constructed by adding layers of materials onto a planar surface as a line or a point, via material extrusion, vat photopolymerization, material or binder jetting, powder bed fusion, sheet lamination, and directed energy deposition.⁵ By 1986, Hull had successfully commercialized their SLA-based 3D printer, which is a refined version of their first printer. The SLA adopts a vat photopolymerization process to convert a liquid plastic (typically acrylate) into a solid object, through a laser scan of liquid photocurable material.^{1, 2} Later, other inventors began to create alternatives to the Hull's UV light-based system. In 1989, following Hull's invention, Deckard developed an alternative method of 3D printing, called selective laser sintering (SLS) method.³⁰ In SLS, a laser is used as the power source to fuse or sinter powdered materials, typically, made of plastic, metal, ceramic, and glass, to create solid 3D objects in a layer-by-layer manner. The powdered materials vary on the targeted 3D object.

Another important 3D printing method, fused deposition modelling (FDM), was invented by Crump in 1988.³¹ FDM, one of the material extrusion technologies, uses a thermoplastic filament feed into a heated nozzle to deposit them on a printing substrate through a layer-by-layer fashion, which extrudes heated plastic filaments through a nozzle to build up objects. FDM-based 3D printers pioneered a new way of manufacturing products since their invention and provided a new method of creating prototypes at a lower cost.

SLA was the first system of additive manufacturing (AM) with high resolution and high printing speed, but nowadays, cost-effective FDM is the most widely used 3D printing method. Despite the rapid advancement in AM, its low printing speed, scalability, and quality have hampered the adaptation of 3D printing in large-scale manufacturing applications. Nevertheless, 3D printing capable of printing complex 3D objects with high customizability has attracted the interest of many researchers, because its feature is extremely useful for rapid prototyping, creating concept models, and manufacturing end-products ready to be sent to the market. Moreover, recent developments in machine learning-based processes, computer-aided design (CAD) software, and in novel materials, ranging from plastic and metals to ceramics and even food products, are further expanding the stage for 3D printing.

Medical researchers discovered that even complex parts of the human body can be created by using biomaterials as inks for 3D printing in the same way. Many advantages of 3D printing in biomedical applications are paving the way for possible one of medical solutions such as transplantation of human tissues or organs for regenerative medicine, and the 3D printing of human tissues and organs has now been an emerging research topic. In 2001, for the first time, the transplantation of a 3D printed organ, a bladder, into a patient was reported by Atala. In order to fabricate the bladder, the researchers used a dome-shaped scaffold with a size of a human bladder constructed from a biodegradable polymer and then coated the patient's own bladder cells layer-by-layer on it using a 3D printer. Two different types of cells used for bioinks were deposited on the scaffold, with urothelial cells on the inside and muscle cells on the outer surface.³² However, the structure of Atala's bladder was quite simple. For the fabrication of other complex organs such as heart and liver, researchers needed a method to mimic the vascular networks for keeping the organs alive.

In 2004, Forgacs et al. used a 3D printer to create tubular structures toward the fabrication of blood vessels and then vascular networks. They constructed 3D biological hollow tubes by culturing cells on an outer surface of the 3D printed hollow tubes.³² Their printer contained three print heads that deposited bioinks onto a gelatin sheet served as the extracellular matrix (ECM). Until 2010, this technology was the basis for the 3D bioprinting company, Organovo. For a decade, 3D bioprinting has been developing and then applying in the fabrication of various artificial biological tissue constructs^{33–40} for various biomedical applications such as tissue regeneration.^{41–44} 3D bioprinting has also been widely used in the fabrication of biomimetic tissue models for studying the pathogenesis of the various disease, identifying and optimizing the potential drugs, and inventing the useful novel medical applications. Because it has emerged as a promising technology to create complex tailor-made biological constructs with desired physical and biological properties and is rapidly growing.

In this review, we introduce and review recent advancements of new materials and 3D printing techniques, developed to address the unfulfilled needs of the conventional 3D printing methodologies, especially in biomedical applications such as printing speed, cell growth feasibility, and complex shape achievement. A comparative study of these materials and technologies with respect to the 3D printing parameters will be provided for selecting a suitable application-based 3D printing methodology. Discussion on prospects of 3D printing materials and technologies will be finally covered.

2. Conventional 3D printing methods for medical applications

Nozzle-based techniques, which deposit the bioink in a layer-by-layer regime, have commonly used as a 3D printing method in biomedical applications to create biological 3D constructs. Primary 3D printing methods for medical applications (inkjet-based, extrusion-based, and light-assisted methods) are illustrated in Figure 2. The most used platform is based on the extrusion method, followed by the light-assisted and inkjet-based printing approaches.^{45–65} All these 3D printing methods can print the scaffolds for cell cultures or biological constructs using cell-laden bioinks. However, there are some differences in the printing resolution, materials, speed, and mechanism among these methods. Sections 2.1–2.3 summarize each feature.

2.1 Inkjet-based 3D printing method

The inkjet-based method is presented in Figure 2a. First inkjet bioprinters were the modified versions of the commercially available benchtop 2D inkjet printers where a few picoliter droplets of the bioink composed of biomaterials or cells mixtures in the cartridge are dispensed on an electronically controlled stage to control the z-axis. In the inkjet-based system, multiple actuation mechanisms are used, such as thermal, piezoelectric, electromagnetic, electrostatic, and acoustic, to produce a precise droplet.

Inkjet-based 3D printing methods have the potential to print at a speed of 100 mm/s order and a minimum resolution of 20–100 μm , typically 20 μm .^{36,66} The nozzle diameter and the physical or chemical properties of the bioink determines the resolution of the printed constructs. Typically, the higher printing resolution can be obtained with a smaller diameter

of nozzle heads. The inkjet-based methods generally require bioinks with viscosity lower than 10 mPa·s but offer relatively fast printing speed compared to other techniques.⁶⁷ However, they provide low cell densities and decreased cell viability⁶⁸ and have problems caused by the inherent inability of the printing head that provides a continuous flow, limiting its capability to 3D print the biological constructs compared to extrusion-based techniques.⁶⁹

2.2 Extrusion-based 3D printing method

Extrusion-based 3D printing methods can control the flow of continuous bioinks and have been more widely employed than inkjet-based methods. The dispensing system, which uses pressure, mechanical, or solenoid valves, is adapted to drive the 3D printing system. Extrusion-based 3D printing methods can print cell-laden biomaterials as bioinks onto a target substrate or material through a layer-by-layer regime (Figure 2b).

In extrusion-based methods, bioinks should have a viscosity in the range of 0.001– 10×10^3 mPa·s.⁷⁰ The wide variety of bioinks, i.e., biomaterials, such as gelatin, alginate, hyaluronic acid (HA), polyethylene glycol (PEG)-based hydrogels, decellularized extracellular matrix (dECM), and cell spheroids are applicable, which makes the extrusion-based methods highly advantageous compared to the other printing methods.^{71–74} However, they have limitations in printing speed and resolution. Their printing speed is in the wide range between 0.1 and 150,000 $\mu\text{m/s}$, typically 10–50 $\mu\text{m/s}$, and the lowest among those three types of printing approaches.^{75, 76, 70} In the case of conventional single nozzle, it requires a long time to create large size tissue constructs with bioinks with good viability. The minimal resolution of 5–100 μm and generally over 100 μm has been reported.⁷⁰ This resolution is difficult to mimic the architecture of native components of body such as microvessels, aligned myofibers, and neuronal networks, etc. In comparison with inkjet-based 3D printing methods, the extrusion-based 3D printing methods can handle bioinks with higher cell densities but provide lower printing speeds and resolution.⁶⁸

2.3 Light-assisted 3D printing method

Compared to the nozzle-based systems, light-assisted 3D printing can offer significant improvements in printing speed and resolution, accompanied with smooth features, different from inkjet-based and extrusion-based 3D printing methods. For light-assisted methods, bioinks with a wide range of viscosities, even fluids, are suitable. This enables us to use a larger range of biomaterials but these are restricted to photo-crosslinkable bioinks, typically composed of synthetic and natural biomaterials with photo-crosslinkable groups; gelatin methacryloyl (GelMA) and poly(ethylene glycol) diacrylate (PEGDA) etc. In addition, to ensure an efficient light penetration depth, which affects the quality of the final constructs and the printing resolution, these biomaterials should be transparent against the light source used.

Two types of light-assisted 3D printing methods; the digital light processing (DLP) method and the two-photon polymerization (TPP) method, respectively, are mainly used to fabricate the biological constructs.

2.3.1 DOPsL 3D printing method—The first light-assisted method, i.e. SLA, was developed by Hull. SLA is performed using a digital micromirror-array device (DMD) and controls an array of up to several millions of micro-sized mirrors independently.^{124, 125} In this method, the construct is created through a layer-by-layer regime where one layer is fabricated and then the printing stage is lowered or raised to create a new layer. The entire layer is cured simultaneously. Based on this method, a dynamic optical projection stereolithography (DOPsL) system, which enables the rapid fabrication of complex 3D constructions has been developed by Zhang et al. (Figure 2c).

The DOPsL method provides a higher printing speed than the other techniques, using a few million micromirror chips simultaneously, which makes it easy to fabricate large-scale complex constructs with submicron resolution. The printing speed reaches 500 mm/s and the printing resolution is as low as ~10 μm .^{126–128} This superior performance enabled the researchers to build complex constructs. Complex tissue constructs with fractal geometries, microfluidic mixing chambers, high-precision microwells, constructed with tuneable Poisson ratios, aligned the cardiac scaffolds, vasculature networks, and liver microarchitectures.^{40,103, 129–135} The DOPsL method has also used a wide variety of photopolymerizable hydrogels; GelMA, PEGDA, and glycidyl methacrylate hyaluronic acid (GMHA) etc., but capable biomaterials are limited to materials can be photopolymerized.

2.3.2 TPP 3D printing method—Another light-assisted method is the TPP 3D printing method, which was developed from SLA as a kind of laser-based direct-writing technique. Laser, typically femtosecond laser, is used to polymerize the photo linkable monomers repeatedly and selectively to generate constructs (Figure 2d).¹³⁶ A femtosecond laser can induce two-photon absorption, which is the basic mechanism of the TP method. In a two-photon absorption process, the simultaneous absorption of the two photons induces the excitation of a molecule to a higher-energy electronic state. The probability that a molecule subjected to two-photon absorption process relies on the square of light intensity of the incident light.¹³⁷ The photons can be confined inside the dimension of the voxel below 1 μm , which enables the printing resolution of TPP to reach only 100 nm.^{136,138, 139} Thus, the TPP is an ideal platform for printing 3D objects with nanoscale to microscale features. The printing speed of the TPP method reaches 20 mm/s, which is much faster than those of the nozzle-based 3D printing methods.¹⁴⁰ TPP also accepts various polymers such as hydrogels, PEGDA, HA, collagen, bovine serum albumin, and laminin as bioinks.^{141–145}

Although light-assisted 3D printing techniques have some limitations in the size of the printable constructs, they are now used in various tissue engineering applications and have great potential for fabricating complex 3D biological constructs within short time.

3. Materials for 3D printing in biomedical applications

Bioinks used in 3D printing in biomedical applications are composed of biomaterials and cells. For 3D printing in biological constructs, biomaterials act as an ECM for cells, providing sufficient structural support and a promising cellular attachment, to pattern the cells and the tissues. They also regulate cellular functions and behaviours. The ideal bioinks should not only be printable, but also be nontoxic and biocompatible to facilitate the

biological behaviour of the seed cells or tissues. In order to sustain the functions of the printed biological tissues, bioinks should fulfil certain characteristics required for each specific 3D printing technique.

3.1 Prerequisite parameters for biomaterials used in 3D printing

There are three main classes of biomaterials utilized in 3D printing: melt-cure polymers, hydrogels, and dECM. For biomaterials adopted in 3D printing, the most important prerequisite parameter is the biocompatibility. Basic cellular functions such as a cell attachment and cell migration should be preserved for these biomaterials. For hydrogel-based biomaterials, it needed photo-initiators to crosslink hydrogels by light exposure such as UV and visible lights, but these photoinitiators should also less affect cell viability. It has been reported that some kind of photo-initiators and monomers show cytotoxicity if left unreacted during crosslinking process of hydrogels. The degradation rate of biomaterials should also be matched with the regeneration rate of tissue in order to offer the sufficient structural support for cell activities to complete tissue regeneration.

The elasticity of hydrogels also affects the attachment and proliferation of cells, which depend on the glass transition state (T_g) of hydrogels. Water-swelling causes a lower polymer glass transition and results in a decreased T_g , $<37^\circ\text{C}$. Subsequently, the hydrogels become to disappear in a rubbery elastic state because the hydrogels are plasticized through the incorporation of excess water molecules. Therefore, the viscoelasticity of the hydrogels might be increased below T_g because the rearrangement of the polymer segments is restricted below T_g . Also, hydrogels are sufficiently water-swollen during cell culturing, they can contain a large number of bioactive molecules that are existing in cell culture media resulting in allowing to improve cellular behaviours such as proliferation, differentiation, and elongation.

For biomaterials used in the extrusion-based methods, another important parameter is a non-Newtonian behaviour, determining the viscosity and flow behaviour of the biomaterials during dispensing. When pressure is applied to the biomaterials during dispensing, they exhibit a variety of responses including shear thinning. Viscosity decreases with the increase in the shear rate. Yucel et al.¹⁴⁶ reported that the shear force reorganizes the conformation of polymer chains in the hydrogel and enhances the alignment of the polymer chains from a randomly-oriented conformation by reducing the viscosity of hydrogels during dispensing, i.e., under shear stress (τ), called shear thinning. Shear-thinning has an impact on high molecular-weight biomaterials. This effect enables the easy dispensing of fluid materials under pressure and causes the fluidic biomaterials to restore their gel state by relaxing their stress.

Because the fluidic event of biomaterials is initiated by yield stress, which is instantaneous stress, the minimum stress should be applied before they are dispensed. The yield stress (γ) affects the shear stress, and the structural network of biomaterials breaks when the applied shear force is greater than the yield stress. The yield stress also helps maintain the homogeneous distribution of cells within the bioink. The yield stress required for specific biomaterials can be estimated by extrapolating the flow curve at a low shear rate (μ) against zero shear rate. The Bingham or modified Bingham equation ($\tau = \tau_B + \mu_B \dot{\gamma}$ or $\tau = \tau_{MB} + \mu$

$MBY + Cy^2$), the simplest of the viscoelastic rheological models, can lead the yield stress.^{146, 157} In the Bingham equations, changes in the yield stress by temperature, chemical concentration, pH in biomaterials directly can be considered.

3.2. Appropriate biomaterials choice

Considering the requirements discussed in Section 3.1, the most important concern in 3D printing for biological constructs is the proper choice of biomaterials, which enables the design of the target tissue scaffolds with desired chemical and physical properties. Table 1 summarizes some biomaterials used in different 3D printing techniques.

3.2.1 Melt-cure polymers—Melt-cure polymers have high mechanical strength and durability and can act as effective structural support for tissues and cells. Typical melt-cure polymers are polycaprolactone (PCL), polylactic acid (PLA), and polyurethane (PU). Compared to PU and PLA, PCL is favourable as scaffolds because of its low melting point of $\sim 60^\circ\text{C}$, which can reduce the temperature-induced cell damage. Several groups have demonstrated the use of PCL in liver-on-a-chip, cartilage reconstruction, bone generation, muscle analogues, and vascular networks.^{36,120, 121, 158} Similarly, PLA and PU have also been used in a heart-on-a-chip and neural tissues such as nerve grafts.^{43,44,78,122,123} However, the melt-cure polymers typically require either high process temperature or use of toxic solvents, which brings a less cytocompatibility with cells than those of other biomaterials. In the printing process, the integration of these melt-cure polymers into cell-supportive hydrogels is also difficult.

3.2.2 Hydrogels—Hydrogels are one of the most important biomaterials since they have inherently contained a large amount of water molecules and show good swelling features. Hydrogels can be categorized into two main classes: (1) naturally-derived hydrogels; collagen, gelatin, HA, and alginate etc., and (2) synthetically-derived hydrogels; PEG, poly(lactic-glycolic) acid (PLGA), and PEGDA etc.

Hydrogels can form gel-like structures through physical, chemical, or enzymatic crosslinking.¹⁵⁹ Either a permanent or a reversible hydrogel is formed depending on the type of the crosslinking states. Typically, irreversible permanent hydrogels are formed by introducing chemical bonds such as the covalent bond. Conversely, physical interactions such as hydrogen bonds and ionic forces produce reversible hydrogels. Although the chemical crosslinking requires post-curing, resultant permanent hydrogels show higher mechanical strength than physically cross-linked reversible hydrogels. However, hydrogels typically lack mechanical strength and shape fidelity, compared to melt-cure polymers. In order to improve their mechanical strength and shape fidelity, the integration of hydrogels with melt-cure polymers such as PCL and PLGA has been investigated.

3.2.2.1 Natural hydrogels: The most commonly utilized natural hydrogels in 3D printing are gelatin, collagen, alginate, and HA. These natural hydrogels are biodegradable and can promise native ECM-like environments required for cellular activities because they have similar mechanical properties and biological activities with natural ECM. Natural hydrogels

also show a defined structural feature and a distinct molecular weight, owing to their biological production methods.

Collagen, as the main component of natural ECM and the most abundant protein in mammalian tissues, has been used in various applications such as a liver-on-a-chip and tissue constructs such as cartilage constructs.^{43,93–95} A partial hydrolysis of collagen causes a helix-to-coil transition and thus produces another soluble protein-based polymer, gelatin. Gelatin exhibits lower antigenicity than collagen¹²³ and also undergoes gelation with a change in temperature. Although it usually remains in the gel state below 37°C, an elevated temperature converts it to a liquid. This characteristic allowed it to be utilized as a sacrificial material for cells to construct organ-on-a-chips such as a liver-on-a-chip.⁴³ After the cell incubation, only liquid gelatin was easily removed at decreased temperature, and then cells remained. Gelatin can also be applied to produce a photopolymerizable hydrogel, GelMA, by the introduction of a methyl acrylate group as a synthetic part, which is a potential hydrogel for 3D printing. GelMA has been extensively utilized in various tissue engineering fields such as organ-on-a-chip and the construction of vascular networks, etc.^{40,103, 98, 104}

Alginate and HA are also used to provide scaffolds for cartilage, chondrocytes, vascular networks with branch structures, skin tissue, and muscle constructs.^{62,82,83–90,91} physical properties of HA can be modified through chemical modifications by PEG, thiolate, and guest-host supramolecular complex etc. to enhance the printability and stability.⁷⁸ Alginate can be modified with RGD motifs to offer a mild 3D printing condition needed for printing human pluripotent stem cells to generate mini-livers.^{163, 164} Other natural hydrogels, matrigel, fibrinogen, thrombin, chitosan, and agarose, are used in drug conversion in the liver tissue^{89,92}, skin and muscle constructs^{35,78,80,100}, high-cell-density bioinks⁸⁹, the reconstruction of cartilage and bones¹⁰¹, and the construction of vascular networks^{39,102}, respectively. However, although natural hydrogels have been widely used for constructing various biological tissues, their main limitations are their relatively low mechanical strength, immunogenicity, and stability compared to synthetic hydrogels.

3.2.2.2 Synthetic hydrogels: In comparison with natural hydrogels, synthetic hydrogels have a well-defined structure, and their properties such as the degradation rate, mechanical strength, and structural characteristics to enhance cell adhesion can be more easily controlled reproducibly.¹⁶⁵ Since the late 1960s, the Poly(2-hydroxyethyl methacrylate) (PHEMA) hydrogel has been widely used as an implantable material. However, currently, the most commonly used synthetic hydrogels are PEG and Pluronic F-127. PEGDA, photo-crosslinkable hydrogel, is generated by the addition of photoinitiators.¹⁶⁶ PEGDA has been utilized in vascular construction^{167,40} and in ear construction as a sacrificial material^{102,103}. Other PEG-based hydrogels; poly-(ethylene glycol) methacrylate (PEGMA) and poly(ethylene glycol)-tetra-acrylate (PEGTA) etc. have also been studied for reconstruction of bone and cartilage, and vascular network construction.^{59,77,90, 105, 106, 108, 109} Pluronic F-127, as a temperature-responsive hydrogel, can be converted to a liquid state at low temperatures. This feature allows their application as a sacrificial material for reconstruction of bone and cartilage, tissue engineering of muscle etc., and construction of vascular channel network.^{77, 59,90,109}

PVA can be photo-crosslinked to fabricate hydrogels and used in vascular tissue and cartilage constructs.^{107, 112} PVA hydrogels typically show a higher mechanical strength than most other synthetic hydrogels. They can also be copolymerized with PEG to produce biodegradable hydrogels, and their degradation rate is between that of the PVA hydrogel and the PEG hydrogel.

3.2.2.3 Hybrid hydrogels: While natural hydrogels possess better compatibility with the cell, synthetic hydrogels have a better processability such as printability and shape fidelity. To utilize these two advantages, hybrids of natural and synthetic hydrogels have been developed. In hybrid hydrogels, synthetic hydrogels enhance the mechanical strength while natural hydrogels retain the cell viability and functionality by offering an ECM microenvironment. A potential technique for fabricating hydrogel bioinks with both high printability and cytocompatibility is hybridization. Yin et al.⁵² mixed gelatin with low-concentration GelMA and reversibly formed hydrogels by changing the bioink temperature to regulate the processability during 3D printing. The hybrid hydrogels showed higher cell compatibility than GelMA hydrogels. PEG and GelMA copolymerized hydrogels have been developed to tune their degradation rate and stiffness profiles.¹¹¹ The PEG-GelMA hydrogels exhibited improved cell viability and attachment compared to PEG hydrogels. Miao et al. developed a hybrid hydrogel composed of PVA-gelatin and PEG. They successfully controlled the modulus strength in the range of 10–100 kPa by changing the concentration of PVA and gelatin and the molecular weight of PVA. They have successfully utilized the hybrid hydrogel in cartilage regeneration.¹¹² Armstrong et al.¹¹⁶ showed that the hybrid hydrogels of alginate and pluronic F-127 can be printed at high resolution using the extrusion method, and effectively crosslinked to produce constructs with high cytocompatibility and long-term structural fidelity. As alternative approaches, synthetic materials such as PCL and polydimethylsiloxane (PDMS) have been deposited as supportive scaffolds and mixed into natural hydrogels such as alginate, collagen, gelatin, and fibrinogen.^{80,117–119, 168, 169, 112}

Selected bioinks made from natural, synthetic, and their hybrid hydrogels used for 3D printing are listed in Table 2. An appropriate biomaterials choice is made by considering a combination of following factors; the used printing method, target biological tissues and constructs, cell types, and the biological processes to apply.^{170, 171} Regardless of the selected bioink, biomaterials have the quick crosslinking ability either by chemical or physical manner in order to form a hydrogel network structure after- or during- the printing of 3D constructs. For instance, further development of water-soluble photoinitiators combined with high UV-visible absorption ability is urgent for 3D printing of hydrogels. Recently, Pawar et al.¹⁷² developed highly efficient water-soluble nanoparticle-based UV curable inks, which allowed the 3D printing of hydrogels in an aqueous solution. The water-soluble nanoparticles were made from 2,4,6-trimethylbenzoyl-diphenylphosphine oxide (TPO). TPO can significantly absorb a UV light from 385 to 420 nm and show an extinction coefficient of as high as $\sim 680 \text{ M}^{-1} \text{ cm}^{-1}$, which is over 300 times compared to that of the commercially available water-soluble photoinitiators such as PIs ($2.25 \text{ M}^{-1} \text{ cm}^{-1}$). An $n \rightarrow \pi^*$ transition in the aroyl-phosphinoyl chromophore with a strong conjugation between the phosphonyl group and the carbon atom of the adjacent carbonyl group is the origin of

their strong long and wavelength absorption. Thus, the polymerization rate is magnificently enhanced. This enabled the 3D printing of hydrogels without adding any solvents.

3.2.3 dECM—The development of a novel biomaterial that enables the creation of complex biomimetic tissues is urgently needed. Most natural biomaterials cannot recreate the complexity of natural ECMs because they only have a single component from natural ECMs and lack important major components include proteoglycans, elastin, growth factors, and cell-binding glycoproteins such as laminin and fibronectin.³⁸ This is insufficient to mimic complex living tissues where a microenvironment with cell-to-cell connection and 3D cellular organization is typical. Consequently, researches have focused on the dECM which derived from living tissues and organs for use in 3D printing as well as tissue engineering and regenerative medicine, as no natural or synthetic biomaterials can recapitulate all the features of natural ECMs.^{173, 174} In the decellularization process to fabricate the dECM, all cellular components are removed from living tissues of organs through a combination manner of chemical, mechanical, and enzymatic treatments, which yield collagen while retaining important components of the native ECMs. Perniconi et al. showed that cellular scaffolds can be explanted from mice and they effectively supported the formation of myofibers.¹⁷⁵ Furthermore, Pati et al. developed bioinks made of the decellularized tissues which derived from pepsin solubilized cartilage, adipose, and cardiac tissues. They also demonstrated the practicability of these tissue-specific dECM as bioinks for use in a nozzle-based 3D printing.¹⁶⁸ In fact, the constructs printed from bioinks made of these dECM exhibited an enhanced functionality of encapsulated mesenchymal stem cells derived from the human inferior turbinate-tissue, human adipose-derived stem cells, and rat myoblasts compared to the bioinks made of collagen. The fabrication of functional skeletal muscle constructs were also reported by other research groups using skeletal-derived dECM bioinks.¹⁷³ The significant increase in the osteogenic genes of human adipose-derived stem cells within dECM-PCL constructs manifested the effectiveness of dECM in bone regeneration compared to that in PCL scaffolds.³⁴ These studies imply the versatility of dECM in 3D printing for creating complex biological tissue constructs with a living tissue and organ-like microenvironment. However, the dECM-based bioinks still have an inferior printing formability such as shape fidelity which should be addressed. The dECM has also inherent ethical usage problems because of its origin.

Other biomaterials such as cell spheroids and tissue strands also have potential for replicating the functions and developing processes of native living tissues and organs. The direct 3D printing of cell spheroids- or tissue strands-laden bioinks has reported through a scaffold-free method.³⁹

4. Novel 3D printing techniques and materials

In this section, we introduce the recent advancements in novel 3D printing techniques and their related materials for biomedical applications. Interdisciplinary research is lying on between the 3D printing techniques and advanced materials. Conventional 3D printing methods construct 3D objects by accumulating a layer. However, typically, these techniques lead to a step structure along the edges, called a stair-step effect. The limitations of speed, geometry, and surface quality exist in the material layering methods. They also have

difficulties creating 3D objects with both complexity and multi-functionality. The core problem is to improve the printability and formability of novel biomaterials without losing their superior features of the original material during 3D printing process, and the production of complex and multi-functional constructs.

4.1 Novel SLA and their materials

Recently, Kelly et al.¹⁷⁶ has developed a novel 3D printing technique that uses computed tomography (CT), called computed axial lithography (CAL). The process of CAL was explained by an image reconstruction procedure of CT, which is a technique widely used in medical imaging and non-destructive testing.^{177, 178} Recent developments in CT for use in cancer treatment provided an intensity-modulated radiation therapy (IMRT) method, which enables the targeted tumour areas of the patient's body to expose a critical radiation dose in 3D.¹⁷⁹ Instead of the patient, a photoresponsive material is subjected to the CT scans in the CAL to obtain stair-step free, smooth, flexible, and complex 3D objects. The researchers used a viscous liquid, made from polymers with photocurable grafts and dissolved oxygen molecules, and designed the materials to react against a certain threshold of patterned light for solidification. The desired 3D shape was formed by projecting light onto the rotating cylinder of the liquid (Figure 3a and 3b).

Using the CAL, the formation of a centimetre-scale geometry can be completed in less than 1 min. They have the potential to produce a large array of geometries with a lateral size of up to ~55 mm within the time range of 30 to 300 s. It is also possible to add new parts into an already existing object, i.e., adding a handle to a metal screwdriver shaft, which is difficult to do using conventional 3D printing techniques. The printing materials do not have to be transparent. Even opaque 3D objects can be created using a dye molecule that absorbs visible light in a wide wavelength range except for the curing wavelength.

Grigoryan et al.¹⁸⁰ also developed versatile photopolymerizable hydrogels, which enable the fabrication of complex 3D objects for projection stereolithography. To date, it has been difficult to create complex 3D transport systems where organs transport blood via bio-physically and bio-chemically entangled complex vascular networks. To solve this problem, they established an intravascular and multivascular design using photopolymerizable hydrogels by incorporating a food dye as a biocompatible photoabsorber (Figure 3b to k). The monolithic transparent hydrogels with intravascular 3D fluid mixers and bicuspid valves were produced in minutes, using polyethylene glycol diacrylate with the food dye. Grigoryan et al. also introduced a hydrogel model of a lung-mimicking air sac with airways which enable the delivery of oxygen to the surrounding blood vessels. Successful implantation of bioprinted constructs including liver cells into mice was also demonstrated.

4.2 Multi-materials 3D printing

Alternatively, Kang et al.³⁶ attempted to solve the challenges in producing 3D complex vascularized cellular networks using multi-material 3D printing systems. An integrated tissue-organ printer (ITOP) system that enables the fabrication of any shapes of human-scale tissue constructs was developed. This system was achieved by designing multi-dispensing systems for extruding and patterning multiple cell-laden hydrogels in a single construct;

poly(ϵ -caprolactone) polymer as a supporting construct and pluronic F-127 hydrogel as a sacrificial layer (Figure 4a–c). They developed multiple materials and techniques; an optimized carrier material capable of positioning cells in the liquid form on distinct locations inside the 3D structure, sophisticated nozzle modules with a resolution of as low as 2 μm for biomaterials and 50 μm for cells, and photo cross-linkable cell-laden hydrogels which have photocurable ability even after cell passage. They simultaneously printed an outer sacrificial acellular hydrogel mould that serves as a supporting layer. The lattice of microchannels permits the diffusion of nutrients and oxygen into the printed tissue constructs. The ITOP successfully generated various 3D constructs with multiple cell types and biomaterials and showed the potential for fabricating various types of vascularized tissues. The fabrication of novel organs-on-chip devices has also been demonstrated by Lind et al.,⁴⁴ who used a multi-material 3D bioprinting system. They designed biocompatible soft material-based functional multiple inks. High conductance and piezo-resistive characteristics of the inks induced the self-assembly into physio-mimetic laminar cardiac tissues. The cardiac microphysiological devices were printed in a single step and applied to study the drug responses and the contractile mechanism of laminar cardiac tissues.

Furthermore, very recently, Skylar-Scott et al. developed an extrusion-based new multi-materials printing technique that allows printing with up to eight different inks within a single nozzle (Figure 4 d–g), called multimaterial multinozzle 3D (MM3D) printing method.¹⁸¹ They designed a printhead with a Y-shaped junction that enables the injection of multiple inks into a single nozzle, where each ink with different viscosities can be adjusted by varying the length of the ink channels. Precisely controlled high-speed pneumatic valves were utilized to achieve rapid and seamless switching between different inks, which drastically enhanced the printing speed. Complex 3D objects can be created in a fraction of the time of conventional extrusion-based techniques. Using the MM3D printing method, a successful fabrication of 3D objects with a centimetre-scale such as foldable origami structures and locomotive soft robots, respectively, composed of two alternating epoxy or silicon inks with different stiffnesses was demonstrated within minutes at a speed of 10–40 mm/s.

4.3 Embedded 3D printing

Embedded 3D printing can provide another potential strategy for obtaining complex tissue-like constructs.^{17,182–185} Initially, this method was demonstrated by Lewis et al. who printed a 3D network of interconnected channels within a matrix composed of an acellular hydrogel and silicone using a viscoelastic, sacrificial ink.¹⁸² After curing the matrices and removing the sacrificial ink, the 3D construct with the interconnected channel network was created. The embedded 3D printing involves extruding a viscoelastic ink into a reservoir with a high plateau shear elastic modulus, a low yield stress, and a photo-crosslink ability. To meet these requirements, they developed a Pluronic F127 triblock copolymer with a hydrophobic poly(propylene oxide) segment and two hydrophilic poly(ethylene oxide) segments as a reservoir, though the chemical modification of the terminal hydroxyl groups of the hydrophilic poly(ethylene oxide) segments with diacrylate groups. Following Lewis's report, Burdick et al. developed another embedded printing strategy based on supramolecular assembly of shear-thinning hydrogel inks through guest-host complexes, where the mixture of two different supramolecular hydrogels, respectively, adamantane modified HA served as

guest and β -cyclodextrin modified HA served as host, was injected into a supporting hydrogel to create cell-laden 3D structures such as spiral and channel.^{185,186, 187} The formation of intermolecular guest-host non-covalent bonds between the adamantane modified HA and cyclodextrin modified HA allowed for the rapid formation of supramolecular assemblies. They also successfully extended this technique for use in biomedical applications such as drug delivery.

Recently, Luo et al. also developed a technique for generating complex, freeform, and liquid 3D architectures using the formulated aqueous two-phase systems (ATPSs).¹⁸⁸ They used a polyethylene oxide matrix and an aqueous bioink made of a long carbohydrate molecule, called dextran (Figure 5a and b). This system provides a tension several orders of magnitude lower tension compared to typical aqueous/organic phases, which suppressed the deformation of printed structures. The aqueous-in-aqueous reconfigurable 3D architectures printed on the interface of the noncovalent membrane could stand for weeks by using the chemical interaction between hydrogen bonding within the polymers. The tailor-made microconstructs with perusable vascular networks were created by separately combining different cells with compartmentalized bioinks and matrices.

For use in the embedded 3D printing, synthetic¹⁸³, and biopolymer^{184, 185} matrices with a viscoplastic response and self-healing features were further studied. Skylar-Scott et al.¹⁸⁹ developed organ building blocks (OBBs) composed of patient-specific-induced pluripotent stem cell (iPSC)-derived organoids and a technique called sacrificial writing into functional tissue (SWIFT). Thousands of OBBs were assembled into the living matrices at high cellular density and introduced them to perfusable vascular channels. The OBB matrices exhibited the desired viscoelastic and self-healing behaviour to allow the rapid therapeutic-scale assembly of patient- and organ-specific tissues (Figure 5c and d).

4.4 4D printing and materials

Tibbit et al.^{44, 190} originally introduced an idea for fabricating complex 3D objects that can react against an external environment stimulus, called the 4D printing method. They discovered one of methods for creating new design systems. The 4D printing method uses stimuli-responsive smart materials instead of conventional materials. This result in the formation of self-assembling and self-regulating constructs, which can change their shape upon external environmental stimuli.^{3,190, 191, 192–198} Currently, many studies focus on the fabrication of 4D printed constructs with shape changing abilities such as bending, twisting, elongating, and corrugating against external stimuli such as temperature, humidity, or light. The feasibility of 4D printing relies on the development of new smart materials, novel printing techniques, and mathematical modelling of deformation mechanisms.

Most-widely studied smart materials for 4D printing are temperature-responsive materials. The deformation mechanism of temperature-responsive materials relies on the shape memory effect.¹⁹⁹ Shape memory polymers (SMPs) are typically used because of their ease of printability and capability of recovering their original shape state under an external stimulus after undergoing deformation. The T_g value of SMPs is typically higher than their operating temperatures. Their shapes can be programmed through subsequent heating ($>T_g$) and cooling ($<T_g$) treatments. When operating temperature is $<T_g$, they adopt a temporary

deformed shape. After the temperature increases to $>T_g$, they return to their original shape.¹⁹⁹ For example, SMP fibres were incorporated into an elastomeric matrix to create a hinge structure.^{200–202} The hinge could bend with a maximum deformation angle of $\sim 20^\circ$. The deformation angle depends on the T_g value of SMPs. Wei et al.²⁰³ fabricated 4D active shape-changing structures by direct-write printing of UV photo cross-linkable poly(lactic acid)-based bioinks (Figure 6a and b) based on the SMPs and shape memory nanocomposites (SMNCs). The printed constructs exhibited superior shape memory behaviour, which allowed 3D-1D-3D, 3D-2D-3D, and 3D-3D-3D configuration transformations. Furthermore, to improve their motion freedom, a six-petal leaf with a bilayer structure that laminates a polylactic acid on paper was fabricated by Zhang et al.²⁰⁴ The bilayer leaves uniformly curled into a flower shape upon changing the environment temperature (Figure 7c–e). This strategy is applicable to creating complex structures with corrugated and helical configurations.

Malachowski et al.²⁰⁵ also reported the fabrication of temperature-responsive multi-fingered grippers. The grippers consist of rigid segments made from poly(propylene fumarate) and stimuli-responsive hinges made from poly(N-isopropylacrylamide-co-acrylic acid) using the stereolithography technique. The grippers grip the drugs at $>32^\circ\text{C}$ and release them onto the targeted tissue at the body temperature of 37°C (Figure 6f–h). The fabrication of the containers made from photoresist panels and thermo-responsive PCL hinges was also demonstrated using photolithography (Figure 6i–l).²⁰⁶ Similar approaches that used temperature as an external stimulus have been reported by several research groups.^{207–209}

Humidity-responsive materials to actuate the deformation by up-taking or releasing the moisture were used for 4D printing.^{206, 210} Initially, 3D objects printed from inks composed of rigid polymers and humidity-responsive materials were demonstrated by Raviv et al.²¹¹ Upon changing the moisture level, the volume of the printed object was extended and folded by 200% from its original state. However, the obtained object was relatively fragile against the repeated motion of folding and unfolding. Mao et al.²¹² printed a structure with the anisotropic swelling properties by confining the hydrogels in one direction using stiff materials. Gladman et al.²¹³ demonstrated a 4D printed structure with four times higher transverse swelling strain characteristics than that of the longitudinal strain using a hydrogel ink, which includes cellulose fibrils. The cellulose fibrils in the hydrogel ink were aligned by the shear forces generated from the contact between the ink and the print bed. Mulakkal et al.²¹⁴ also fabricated humidity-responsive natural hydrogel constructs using carboxymethyl cellulose hydrocolloids. Zhang et al.²¹⁵ designed a hydrogel construct with quick response properties by using hydrophobic thin films derived from cellulose stearoyl esters (CSEs). Their actuation properties could control the changes in the temperature of the surrounding aqueous environment. Other research groups have also developed soft actuators, humidity-responsive sensors, and drug delivery systems by using humidity-responsive hydrogels (e.g., PEGDA) and biodegradable elastomers (e.g., poly(glycerol sebacate)).^{216, 217–219}

The use of light-responsive materials offers a basis to develop novel stimuli-responsive constructs and printing techniques because light as a stimulus has the ability to focus the energy only on the desired area, enabling a rapid and local control or switching of the light-responsive materials. The photoresponsive material is locally heated by the absorbing light.

Yang et al.²²⁰ demonstrated light-responsive sunflower-like 3D objects composed of carbon black and PU-based SMP with sequential bud-to-bloom deformation driven by heat generated from absorbed light. On this mechanism, light was utilized for the deformation of various self-folding structures.^{221, 222, 223} Wu et al.²²⁴ demonstrated the versatility of the light sources as external stimuli for patterning the bent 4D printed constructs. The drug delivery system has also been developed using the poly(lactic-co-glycolic) acid capsule loaded with plasmonic gold nanorods.²²⁵ In this system, the capsule is ruptured by laser irradiation with the resonance wavelength of the gold nanorods.

Electric and magnetic fields can also be used in 4D printing as heat sources. A soft artificial muscle made from a mixture of silicone elastomer and ethanol was reported by Miriyev et al.²²⁶ They used a phase shift characteristic from the liquid state to the gas state in ethanol under the applied current to control the volume of the silicon elastomer matrix. Okuzaki et al.²²⁷ used polypyrrole (PPy) films to create an origami microrobot, which can be controlled by changing the water absorption or the desorption state through an on/off current. Incorporation of magnetic nanoparticles into a hydrogel-based microgripper successfully allowed them to control the microrobot remotely by applying magnetic fields.²¹⁶ Kim et al.²²⁸ demonstrated the fabrication of silicon rubber-neodymium-iron-boron (NdFeB) hybrid 3D structures with programmed ferromagnetic domains by applying a magnetic field during printing. They also showed a shape change by magnetic actuation. Apart from the physical stimuli such as temperature and light, chemical stimuli (pH and ionic concentration) and biological stimuli (glucose and enzymes) have also attracted much interest for the advancement of 4D printing and their related materials and opened a path for constructing new biomedical devices.²²⁹

As described above, 4D printed constructs have the capability of changing their shape and functionality with time. This time-dependent shape-change ability can provide tremendous potential applications for use in biomedical actuators such as self-bending/tightening valves, staples, and stents, biomedical microrobots to deliver and release drugs upon external stimulation for targeted therapy, and biosensors for medical diagnostics. Another intriguing application is the fabrication of scaffolds for tissue regeneration, which allows the scaffolds to mimic the complexity of human tissues that possess a dynamic change in their tissue conformations during the tissue regeneration process. 4D printed tissue constructs with a response to fluctuations in the external environment and geometry change can offer a favourable dynamic microenvironment for tissue regeneration that could not be precisely mimicked in conventional 3D printed tissue constructs.

4.5 Electrically controlled 3D printing

Yang et al. made progress for creating 3D hierarchical architectures which mimicked a natural nacre by developing a novel electrically assisted 3D printing technique.^{230, 231} Their method enabled the fabrication of complex 3D constructs with superior mechanical and electrical properties. They used 3-aminopropyltriethoxysilane grafted graphene nanoplates (GNs) whose thickness is ~8 nm, diameter is ~25 μm , and surface area is as large as ~120 to 150 m^2/g , to strengthen the interface with the polymer matrix (epoxy diacrylate and glycol diacrylate). The concept of their 3D printing system with electrically assistance is shown in

Figure 7a. The electric field of 433 V/cm was applied to align GNs in the polymer matrix during the printing process. GNs in a dielectric polymer ink are polarized under the electric field and gain higher dipole moment in the parallel direction to the platelet of GN because of the shape anisotropy in GN, resulting in the alignment of GNs (Figure 7b). Their superior mechanical toughness of 1.59 MPa m^{1/2} is originating from the synergistic effects of the hydrogen bonding and π - π interaction between the GNs and the polymer and the covalent Si-O-Si bonding between the aminopropyltriethoxysilane grafts on GNs. This technique is promising for designing and creating a lightweight and strong smart object for use in not only biomedical applications but also transportation, aerospace, and military applications.

Wang et al. also proposed a novel method for patterning liquid hydrogels with a resolution of as low as 100 μ m by introducing a capacitor edge effect, called PLEEC. The PLEEC system consists of five layers (Figure 7c-f): a pair of silver adhesive electrodes isolated by a dielectric polyimide film layer, an insulating bottom acrylate film layer, and a top Teflon film layer that acts as an insulator to preserve the liquidous hydrogels on the top of surface isolated from the upper electrode.²³² The top layer should be hydrophobic to send any liquid hydrogels away when the electric field is off. Upon applying the electric field, an electrostatic force is generated to trap the liquidous hydrogels on the top of the surface layer by the capacitor edge effect.

The printed hydrogel objects could effectively respond to the environment temperature. They also demonstrated the fabrication and the operation of the ionic high-integrity hydrogel display device. Current 3D printing techniques using hydrogels as ink largely relies on the physical and chemical properties of hydrogels that have some constraints on their formability. However, their PLEEC system combined the 3D patterning and stacking processes of hydrogels to offer great opportunities in rapid fabrication of prototype hydrogel constructs with complex geometries and devices with multiple components.

Conclusions

3D printing techniques have been receiving growing attention for use in medical applications because of their robust capabilities to produce biomimetic biological structures with ease. This review summarized the conventional and recent advances in 3D printing techniques and materials in biomedical applications. Current technological challenges for 3D printing technologies exist for the strategies to achieve higher resolution, higher printing speed, and larger scale while retaining good biocompatibility. Conventional 3D printing techniques have already demonstrated success in generating biological constructs such as a cartilage, bone, heart, brain, and muscle, but achieving complex, reproducible, large biological constructs with vascularized architectures which suitable for biomedical applications has proved to be challenging. Recent light-assist based 3D printing techniques, computed axial lithography (CAL), showed promising potential for achieving a microscale resolution and a speed up to \sim 1 mm/s. The combination of such projection stereolithography and dye-added photopolymerizable hydrogels also enabled the fabrication of a lung-mimicking air sac with airways that enable the delivery of oxygen molecules into surrounding blood vessels. The constructs containing liver cells are successfully implanted into mice. The recently developed, the integrated tissue-organ printer (ITOP) technique also has a potential to

produce large-scale biological tissue constructs with a complex geometry, human-scale, and high structural integrity. The ITOP was found feasible to create sizable biological constructs that mimicked the structure of native living tissues; human ear-shaped tissue constructs integrated with cartilage tissues, vascularized functional constructs, and skeletal muscle constructs. Embedded 3D printing techniques also have the potential to obtain complex tissue-like constructs. There remain some challenges, but these technologies greatly advance the field of tissue engineering.

Development of novel biomaterials merged with the desired mechanical properties and high cytocompatibilities, which can recapitulate the extracellular environment, is urgent for 3D printing in biomedical applications. There are still great limitations on the variety of biomaterials can be applicable for conventional 3D printing in biomedical applications. Because of the prerequisite parameters on biomaterials to possess the specific features of biocompatibility and formability, the hydrogels are commonly used as biomaterials for obtaining biological 3D constructs. Therefore, towards the fabrication of complex 3D functional tissues or organs using 3D printing techniques, efforts have been made to develop multi-functional biomaterials and bioinks that can mimic natural ECM. For mimicking a natural ECM, an application of decellularized ECM into 3D printing of biological constructs using extrusion-based and light-assisted methods has been studied. The dECM-based bioinks have heterogeneous constituents such as cell-binding proteins and growth factors presented in the ECM of native tissue compared to natural hydrogels that are highly purified forms of single ECM component, which enabled researchers to create patient- and organ-specific cell-laden constructs possess native ECM-like microenvironments. This strategy is useful for developing 3D printed biological tissues and organs because the dECM has the potential to modulate biological activities such as cell proliferation, differentiation, migration, and maturation. However, there are still problems with the printing shape fidelity and ethics for its widespread use in 3D printing. Recently developed, multi-functional biomaterials such as stimuli-responsive hydrogels and reversible crosslinking polymers for 4D printing are also promising for creating programmed 3D constructs with complex geometries for biomedical applications and new design systems. The future of biomaterials and biomaterials-based 3D/4D printing is bright. Further improvements in biomaterials and printing technologies will promise the fabrication and engineering of tailor-made functional 3D biological constructs with more complex geometries and artificial organs.

Acknowledgements

This paper was funded by the National Institutes of Health (R01AR074234, R21EB026824, and R01AR073822-01), the Brigham Research Institute Stepping Strong Innovator Award, and AHA Innovative Project Award (19IPL0I34660079).

References

1. Hull CW, US Patent: 4575330 A, 1989.
2. Heller TB, Patent: WO 1991012120A1, 1990.
3. Choi J, Kwon OC, Jo W, Lee HJ and Moon M-W, 3D Printing and Additive Manufacturing, 2015, 2, 159–167.
4. Dinda GP, Dasgupta AK and Mazumder J, Scripta Materialia, 2012, 67, 503–506.

5. Yeo J, Jung GS, Martin-Martinez FJ, Ling S, Gu GX, Qin Z and Buehler MJ, *Phys Scr*, 2018, 93, 053003. [PubMed: 31866694]
6. Gao W, Zhang Y, Ramanujan D, Ramani K, Chen Y, Williams CB, Wang CCL, Shin YC, Zhang S and Zavattieri PD, *Computer-Aided Design*, 2015, 69, 65–89.
7. Edgar J and Tint S, *Johnson Matthey Technology Review*, 2015, 59, 193–198.
8. Gu GX and Buehler MJ, *Acta Mechanica*, 2018, 229, 4033–4044.
9. Libonati F, Gu GX, Qin Z, Vergani L and Buehler MJ, *Advanced Engineering Materials*, 2016, 18, 1354–1363.
10. Melchels FPW, Domingos MAN, Klein TJ, Malda J, Bartolo PJ and Huttmacher DW, *Progress in Polymer Science*, 2012, 37, 1079–1104.
11. Gu BK, Choi DJ, Park SJ, Kim MS, Kang CM and Kim CH, *Biomater Res*, 2016, 20, 12. [PubMed: 27114828]
12. Compton BG and Lewis JA, *Adv Mater*, 2014, 26, 5930–5935. [PubMed: 24942232]
13. Wegst UG, Bai H, Saiz E, Tomsia AP and Ritchie RO, *Nat Mater*, 2015, 14, 23–36. [PubMed: 25344782]
14. Ligon SC, Liska R, Stampfl J, Gurr M and Mulhaupt R, *Chem Rev*, 2017, 117, 10212–10290. [PubMed: 28756658]
15. Gu GX, Takaffoli M and Buehler MJ, *Adv Mater*, 2017, 29, 1700060.
16. Norman J, Madurawe RD, Moore CM, Khan MA and Khairuzzaman A, *Adv Drug Deliv Rev*, 2017, 108, 39–50. [PubMed: 27001902]
17. Wehner M, Truby RL, Fitzgerald DJ, Mosadegh B, Whitesides GM, Lewis JA and Wood RJ, *Nature*, 2016, 536, 451–455. [PubMed: 27558065]
18. Sullivan TN, Pissarenko A, Herrera SA, Kisailus D, Lubarda VA and Meyers MA, *Acta Biomater*, 2016, 41, 27–39. [PubMed: 27184403]
19. Uzel SG, Platt RJ, Subramanian V, Pearl TM, Rowlands CJ, Chan V, Boyer LA, So PT and Kamm RD, *Sci Adv*, 2016, 2, e1501429. [PubMed: 27493991]
20. Zhang B, Gao L, Ma L, Luo Y, Yang H and Cui Z, *Engineering*, 2019, 5, 777–794.
21. Gaynor AT, Meisel NA, Williams CB and Guest JK, *Journal of Manufacturing Science and Engineering*, 2014, 136, 061015.
22. Zegard T and Paulino GH, *Structural and Multidisciplinary Optimization*, 2015, 53, 175–192.
23. Gu GX, Takaffoli M, Hsieh AJ and Buehler MJ, *Extreme Mechanics Letters*, 2016, 9, 317–323.
24. Gu GX, Chen C-T, Richmond DJ and Buehler MJ, *Materials Horizons*, 2018, 5, 939–945.
25. Gu GX, Wettermark S and Buehler MJ, *Additive Manufacturing*, 2017, 17, 47–54.
26. Jared BH, Aguilo MA, Beghini LL, Boyce BL, Clark BW, Cook A, Kaehr BJ and Robbins J, *Scripta Materialia*, 2017, 135, 141–147.
27. Capel AJ, Rimington RP, Lewis MP and Christie SDR, *Nature Reviews Chemistry*, 2018, 2, 422–436.
28. Peppas NA, Hilt JZ, Khademhosseini A and Langer R, *Advanced Materials*, 2006, 18, 1345–1360.
29. Holmes B, Zhu W, Li J, Lee JD and Zhang LG, *Tissue Eng Part A*, 2015, 21, 403–415. [PubMed: 25088966]
30. Deckard CR, US Patent: 4863538, 1986.
31. Hamzah HH, Shafiee SA, Abdalla A and Patel BA, *Electrochemistry Communications*, 2018, 96, 27–31.
32. Blohm CE, ReferencePoint Press, 2018.
33. Dolati F, Yu Y, Zhang Y, De Jesus AM, Sander EA and Ozbolat IT, *Nanotechnology*, 2014, 25, 145101. [PubMed: 24632802]
34. Choi YJ, Kim TG, Jeong J, Yi HG, Park JW, Hwang W and Cho DW, *Adv Healthc Mater*, 2016, 5, 2636–2645. [PubMed: 27529631]
35. Cubo N, Garcia M, Del Canizo JF, Velasco D and Jorcano JL, *Biofabrication*, 2016, 9, 015006. [PubMed: 27917823]
36. Kang HW, Lee SJ, Ko IK, Kengla C, Yoo JJ and Atala A, *Nat Biotechnol*, 2016, 34, 312–319. [PubMed: 26878319]

37. Morimoto Y, Onoe H and Takeuchi S, *Science Robotics*, 2018, 3, eaat4440. [PubMed: 33141706]
38. Kolesky DB, Homan KA, Skylar-Scott MA and Lewis JA, *Proc Natl Acad Sci U S A*, 2016, 113, 3179–3184. [PubMed: 26951646]
39. Norotte C, Marga FS, Niklason LE and Forgacs G, *Biomaterials*, 2009, 30, 5910–5917. [PubMed: 19664819]
40. Zhu W, Qu X, Zhu J, Ma X, Patel S, Liu J, Wang P, Lai CS, Gou M, Xu Y, Zhang K and Chen S, *Biomaterials*, 2017, 124, 106–115. [PubMed: 28192772]
41. Bhise NS, Manoharan V, Massa S, Tamayol A, Ghaderi M, Miscuglio M, Lang Q, Shrike Zhang Y, Shin SR, Calzone G, Annabi N, Shupe TD, Bishop CE, Atala A, Dokmeci MR and Khademhosseini A, *Biofabrication*, 2016, 8, 014101. [PubMed: 26756674]
42. Fu F, Chen Z, Zhao Z, Wang H, Shang L, Gu Z and Zhao Y, *Proc Natl Acad Sci U S A*, 2017, 114, 5900–5905. [PubMed: 28533368]
43. Lee H and Cho DW, *Lab Chip*, 2016, 16, 2618–2625. [PubMed: 27302471]
44. Lind JU, Busbee TA, Valentine AD, Pasqualini FS, Yuan H, Yadid M, Park SJ, Kotikian A, Nesmith AP, Campbell PH, Vlassak JJ, Lewis JA and Parker KK, *Nat Mater*, 2017, 16, 303–308. [PubMed: 27775708]
45. Bertlein S, Brown G, Lim KS, Jungst T, Boeck T, Blunk T, Tessmar J, Hooper GJ, Woodfield TBF and Groll J, *Adv Mater*, 2017, 29, 1703404.
46. Liu W, Zhang YS, Heinrich MA, De Ferrari F, Jang HL, Bakht SM, Alvarez MM, Yang J, Li YC, Trujillo-de Santiago G, Miri AK, Zhu K, Khoshakhlagh P, Prakash G, Cheng H, Guan X, Zhong Z, Ju J, Zhu GH, Jin X, Shin SR, Dokmeci MR and Khademhosseini A, *Adv Mater*, 2017, 29, 1604630.
47. Xu C, Lee W, Dai G and Hong Y, *ACS Appl Mater Interfaces*, 2018, 10, 9969–9979. [PubMed: 29451384]
48. Liu W, Heinrich MA, Zhou Y, Akpek A, Hu N, Liu X, Guan X, Zhong Z, Jin X, Khademhosseini A and Zhang YS, *Adv Healthc Mater*, 2017, 6, 1601451.
49. Apelgren P, Amoroso M, Lindahl A, Brantsing C, Rotter N, Gatenholm P and Kolby L, *PLoS One*, 2017, 12, e0189428. [PubMed: 29236765]
50. Wu Z, Su X, Xu Y, Kong B, Sun W and Mi S, *Sci Rep*, 2016, 6, 24474. [PubMed: 27091175]
51. Byambaa B, Annabi N, Yue K, Trujillo-de Santiago G, Alvarez MM, Jia W, Kazemzadeh-Narbat M, Shin SR, Tamayol A and Khademhosseini A, *Adv Healthc Mater*, 2017, 6, 1700015.
52. Yin J, Yan M, Wang Y, Fu J and Suo H, *ACS Appl Mater Interfaces*, 2018, 10, 6849–6857. [PubMed: 29405059]
53. Gu Q, Tomaskovic-Crook E, Wallace GG and Crook JM, *Adv Healthc Mater*, 2017, 6, 1700175.
54. Wang Z, Jin X, Tian Z, Menard F, Holzman JF and Kim K, *Adv Healthc Mater*, 2018, 7, e1701249. [PubMed: 29405607]
55. Dinh ND, Luo R, Christine MTA, Lin WN, Shih WC, Goh JC and Chen CH, *Small*, 2017, 13, 1700684.
56. Keriquel V, Oliveira H, Remy M, Ziane S, Delmond S, Rousseau B, Rey S, Catros S, Amedee J, Guillemot F and Fricain JC, *Sci Rep*, 2017, 7, 1778. [PubMed: 28496103]
57. Zhang Z, Xiong R, Mei R, Huang Y and Chrisey DB, *Langmuir*, 2015, 31, 6447–6456. [PubMed: 26011320]
58. Sakai S, Kamei H, Mori T, Hotta T, Ohi H, Nakahata M and Taya M, *Biomacromolecules*, 2018, 19, 672–679. [PubMed: 29393630]
59. Gao G, Schilling AF, Hubbell K, Yonezawa T, Truong D, Hong Y, Dai G and Cui X, *Biotechnol Lett*, 2015, 37, 2349–2355. [PubMed: 26198849]
60. Khanmohammadi M, Dastjerdi MB, Ai A, Ahmadi A, Godarzi A, Rahimi A and Ai J, *Biomater Sci*, 2018, 6, 1286–1298. [PubMed: 29714366]
61. Christensen K, Xu C, Chai W, Zhang Z, Fu J and Huang Y, *Biotechnol Bioeng*, 2015, 112, 1047–1055. [PubMed: 25421556]
62. Hart LR, Li S, Sturgess C, Wildman R, Jones JR and Hayes W, *ACS Appl Mater Interfaces*, 2016, 8, 3115–3122. [PubMed: 26766139]
63. Samson AAS, Lee J and Song JM, *Sci Rep*, 2018, 8, 591. [PubMed: 29330381]

64. Tse CCW and Smith PJ, *Methods Mol Biol*, 2018, 1771, 107–117. [PubMed: 29633208]
65. Hendriks J, Willem Visser C, Henke S, Leijten J, Saris DB, Sun C, Lohse D and Karperien M, *Sci Rep*, 2015, 5, 11304. [PubMed: 26065378]
66. Ma X, Liu J, Zhu W, Tang M, Lawrence N, Yu C, Gou M and Chen S, *Adv Drug Deliv Rev*, 2018, 132, 235–251. [PubMed: 29935988]
67. Gudapati H, Dey M and Ozbolat I, *Biomaterials*, 2016, 102, 20–42. [PubMed: 27318933]
68. Holzl K, Lin S, Tytgat L, Van Vlierberghe S, Gu L and Ovsianikov A, *Biofabrication*, 2016, 8, 032002. [PubMed: 27658612]
69. Ozbolat IT and Yu Y, *IEEE Trans Biomed Eng*, 2013, 60, 691–699. [PubMed: 23372076]
70. Ozbolat IT, Moncal KK and Gudapati H, *Additive Manufacturing*, 2017, 13, 179–200.
71. Jia W, Gungor-Ozkerim PS, Zhang YS, Yue K, Zhu K, Liu W, Pi Q, Byambaa B, Dokmeci MR, Shin SR and Khademhosseini A, *Biomaterials*, 2016, 106, 58–68. [PubMed: 27552316]
72. Graham AD, Olof SN, Burke MJ, Armstrong JPK, Mikhailova EA, Nicholson JG, Box SJ, Szele FG, Perriman AW and Bayley H, *Sci Rep*, 2017, 7, 7004. [PubMed: 28765636]
73. Ozbolat IT and Hospodiuk M, *Biomaterials*, 2016, 76, 321–343. [PubMed: 26561931]
74. Axpe E and Oyen ML, *Int J Mol Sci*, 2016, 17, 1976.
75. Langer R and Vacanti JP, *Science*, 1993, 260, 920–926. [PubMed: 8493529]
76. de Grujil FR, van Kranen HJ and Mullenders LHF, *Journal of Photochemistry and Photobiology B: Biology*, 2001, 63, 19–27.
77. Momeni F, Mehdi Hassani SM, Liu N, X and Ni J, *Materials & Design*, 2017, 122, 42–79.
78. Merceron TK, Burt M, Seol YJ, Kang HW, Lee SJ, Yoo JJ and Atala A, *Biofabrication*, 2015, 7, 035003. [PubMed: 26081669]
79. Hsieh FY, Lin HH and Hsu SH, *Biomaterials*, 2015, 71, 48–57. [PubMed: 26318816]
80. Huang Y, He K and Wang X, *Mater Sci Eng C Mater Biol Appl*, 2013, 33, 3220–3229. [PubMed: 23706204]
81. Hung KC, Tseng CS, Dai LG and Hsu SH, *Biomaterials*, 2016, 83, 156–168. [PubMed: 26774563]
82. Xu T, Zhao W, Zhu JM, Albanna MZ, Yoo JJ and Atala A, *Biomaterials*, 2013, 34, 130–139. [PubMed: 23063369]
83. Xu C, Chai W, Huang Y and Markwald RR, *Biotechnol Bioeng*, 2012, 109, 3152–3160. [PubMed: 22767299]
84. Ozbolat IT, Chen H and Yu Y, *Robotics and Computer-Integrated Manufacturing*, 2014, 30, 295–304.
85. Ahn S, Lee H and Kim G, *Carbohydr Polym*, 2013, 98, 936–942. [PubMed: 23987431]
86. Lee H, Ahn S, Bonassar LJ, Chun W and Kim G, *Tissue Eng Part C Methods*, 2013, 19, 784–793. [PubMed: 23469894]
87. Poldervaart MT, Goversen B, de Ruijter M, Abbadessa A, Melchels FPW, Oner FC, Dhert WJA, Vermonden T and Alblas J, *PLoS One*, 2017, 12, e0177628. [PubMed: 28586346]
88. Shim J-H, Lee J-S, Kim JY and Cho D-W, *Journal of Micromechanics and Microengineering*, 2012, 22, 085014.
89. Guillotin B, Souquet A, Catros S, Duocastella M, Pippenger B, Bellance S, Bareille R, Remy M, Bordenave L, Amedee J and Guillemot F, *Biomaterials*, 2010, 31, 7250–7256. [PubMed: 20580082]
90. Pallab Datta AD, Yu Yin, Hayes Dan, Gudapati Hemanth and Ozbolat Ibrahim T., *International Journal of Bioprinting*, 2017, 3, 109–120.
91. You F, Eames BF and Chen X, *Int J Mol Sci*, 2017, 18, 1597.
92. Snyder JE, Hamid Q, Wang C, Chang R, Emami K, Wu H and Sun W, *Biofabrication*, 2011, 3, 034112. [PubMed: 21881168]
93. Rhee S, Puetzer JL, Mason BN, Reinhart-King CA and Bonassar LJ, *ACS Biomaterials Science & Engineering*, 2016, 2, 1800–1805.
94. Yoo WLVKLSPKFJ-HLJ-KPS-S, *TRANSDUCERS 2009 – 2009 International Solid-State Sensors, Actuators and Microsystems Conference*, 2009, DOI: 10.1109/SENSOR.2009.5285591, 10916916.

95. Michael S, Sorg H, Peck CT, Koch L, Deiwick A, Chichkov B, Vogt PM and Reimers K, *PLoS One*, 2013, 8, e57741. [PubMed: 23469227]
96. Wang X, Yan Y, Pan Y, Xiong Z, Liu H, Cheng J, Liu F, Lin F, Wu R, Zhang R and Lu Q, *Tissue Eng*, 2006, 12, 83–90. [PubMed: 16499445]
97. Schiele NR, Chrisey DB and Corr DT, *Tissue Eng Part C Methods*, 2011, 17, 289–298. [PubMed: 20849381]
98. Visser J, Peters B, Burger TJ, Boomstra J, Dhert WJ, Melchels FP and Malda J, *Biofabrication*, 2013, 5, 035007. [PubMed: 23817739]
99. Skardal A, Zhang J and Prestwich GD, *Biomaterials*, 2010, 31, 6173–6181. [PubMed: 20546891]
100. Ng WL, Yeong WY and Naing MW, *Procedia CIRP*, 2016, 49, 105–112.
101. Malafaya PB and Reis RL, *Acta Biomater*, 2009, 5, 644–660. [PubMed: 18951857]
102. Bertassoni LE, Cecconi M, Manoharan V, Nikkiah M, Hjortnaes J, Cristino AL, Barabaschi G, Demarchi D, Dokmeci MR, Yang Y and Khademhosseini A, *Lab Chip*, 2014, 14, 2202–2211. [PubMed: 24860845]
103. Ma X, Qu X, Zhu W, Li YS, Yuan S, Zhang H, Liu J, Wang P, Lai CS, Zanella F, Feng GS, Sheikh F, Chien S and Chen S, *Proc Natl Acad Sci U S A*, 2016, 113, 2206–2211. [PubMed: 26858399]
104. Soman P, Chung PH, Zhang AP and Chen S, *Biotechnol Bioeng*, 2013, 110, 3038–3047. [PubMed: 23686741]
105. Lee JS, Hong JM, Jung JW, Shim JH, Oh JH and Cho DW, *Biofabrication*, 2014, 6, 024103. [PubMed: 24464765]
106. Zhang Z, Jin Y, Yin J, Xu C, Xiong R, Christensen K, Ringeisen BR, Chrisey DB and Huang Y, *Applied Physics Reviews*, 2018, 5, 041304.
107. Chaouat M, Le Visage C, Baille WE, Escoubet B, Chaubet F, Mateescu MA, A Letourneur D, *Adv. Funct. Mater.* 2008, 18, 2855–2861.
108. Chan V, Zorlutuna P, Jeong JH, Kong H and Bashir R, *Lab Chip*, 2010, 10, 2062–2070. [PubMed: 20603661]
109. Kolesky DB, Truby RL, Gladman AS, Busbee TA, Homan KA and Lewis JA, *Adv Mater*, 2014, 26, 3124–3130. [PubMed: 24550124]
110. Wang Z, Abdulla R, Parker B, Samanipour R, Ghosh S and Kim K, *Biofabrication*, 2015, 7, 045009. [PubMed: 26696527]
111. Hutson CB, Nichol JW, Aubin H, Bae H, Yamanlar S, Al-Haque S, Koshy ST and Khademhosseini A, *Tissue Eng Part A*, 2011, 17, 1713–1723. [PubMed: 21306293]
112. Miao T, Miller EJ, McKenzie C and Oldinski RA, *Journal of Materials Chemistry B*, 2015, 3, 9242–9249. [PubMed: 32262923]
113. Kim JE, Kim SH and Jung Y, *Tissue Eng Regen Med*, 2016, 13, 636–646. [PubMed: 30603445]
114. Jang J, Park JY, Gao G and Cho DW, *Biomaterials*, 2018, 156, 88–106. [PubMed: 29190501]
115. Muller M, Becher J, Schnabelrauch M and Zenobi-Wong M, *Biofabrication*, 2015, 7, 035006. [PubMed: 26260872]
116. Armstrong JP, Burke M, Carter BM, Davis SA and Perriman AW, *Adv Healthc Mater*, 2016, 5, 1724–1730. [PubMed: 27125336]
117. Schuurman W, Khristov V, Pot MW, van Weeren PR, Dhert WJ and Malda J, *Biofabrication*, 2011, 3, 021001. [PubMed: 21597163]
118. Shim JH, Kim JY, Park M, Park J and Cho DW, *Biofabrication*, 2011, 3, 034102. [PubMed: 21725147]
119. Xu T, Binder KW, Albanna MZ, Dice D, Zhao W, Yoo JJ and Atala A, *Biofabrication*, 2013, 5, 015001. [PubMed: 23172542]
120. Hung BP, Naved BA, Nyberg EL, Dias M, Holmes CA, Elisseeff JH, Dorafshar AH and Grayson WL, *ACS Biomater Sci Eng*, 2016, 2, 1806–1816. [PubMed: 27942578]
121. Yu Y, Moncal KK, Li J, Peng W, Rivero I, Martin JA and Ozbolat IT, *Sci Rep*, 2016, 6, 28714. [PubMed: 27346373]
122. Duan B, *Ann Biomed Eng*, 2017, 45, 195–209. [PubMed: 27066785]

123. Owens CM, Marga F, Forgacs G and Heesch CM, *Biofabrication*, 2013, 5, 045007. [PubMed: 24192236]
124. Hribar KC, Soman P, Warner J, Chung P and Chen S, *Lab Chip*, 2014, 14, 268–275. [PubMed: 24257507]
125. Lu Y, Mapili G, Suhali G, Chen S and Roy K, *J Biomed Mater Res A*, 2006, 77, 396–405. [PubMed: 16444679]
126. Zhang W, Han L-H and Chen S, *Journal of Manufacturing Science and Engineering*, 2010, 132, 030907.
127. Zhang AP, Qu X, Soman P, Hribar KC, Lee JW, Chen S and He S, *Adv Mater*, 2012, 24, 4266–4270. [PubMed: 22786787]
128. Tumbleston JR, Shirvanyants D, Ermoshkin N, Januszewicz R, Johnson AR, Kelly D, Chen K, Pinschmidt R, Rolland JP, Ermoshkin A, Samulski ET and DeSimone JM, *Science*, 2015, 347, 1349–1352. [PubMed: 25780246]
129. Hribar KC, Finlay D, Ma X, Qu X, Ondeck MG, Chung PH, Zanella F, Engler AJ, Sheikh F, Vuori K and Chen SC, *Lab Chip*, 2015, 15, 2412–2418. [PubMed: 25900329]
130. Liu J, Hwang HH, Wang P, Whang G and Chen S, *Lab Chip*, 2016, 16, 1430–1438. [PubMed: 26980159]
131. Grogan SP, Chung PH, Soman P, Chen P, Lotz MK, Chen S and D’Lima DD, *Acta Biomater*, 2013, 9, 7218–7226. [PubMed: 23523536]
132. Arcaute BKMK, Wicker RB, Springer, 2011, DOI: 10.1007/978-0-387-92904-0.
133. Lee JW, Soman P, Park JH, Chen S and Cho DW, *PLoS One*, 2016, 11, e0155681. [PubMed: 27232181]
134. Skoog SA, Goering PL and Narayan RJ, *J Mater Sci Mater Med*, 2014, 25, 845–856. [PubMed: 24306145]
135. Warner J, Soman P, Zhu W, Tom M and Chen S, *ACS Biomaterials Science & Engineering*, 2016, 2, 1763–1770. [PubMed: 33440474]
136. Park SH, Yang DY and Lee KS, *Laser & Photonics Review*, 2009, 3, 1–11.
137. Cumpston B, Ananthavel S, Barlow S et al., *Nature*, 1999, 398, 51–54.
138. Zipfel WR, Williams RM and Webb WW, *Nat Biotechnol*, 2003, 21, 1369–1377. [PubMed: 14595365]
139. Farsari M and Chichkov BN, *Nature Photonics*, 2009, 3, 450–452.
140. Perevoznik D, Nazir R, Kiyani R, Kurselis K, Koszarna B, Gryko DT and Chichkov BN, *Opt Express*, 2019, 27, 25119–25125. [PubMed: 31510390]
141. Jang T-S, Jung H-D, Pan HM, Han WT, Chen S and Song J, *International Journal of Bioprinting*, 2018, 4, 126. [PubMed: 33102909]
142. Wylie RG, Ahsan S, Aizawa Y, Maxwell KL, Morshead CM and Shoichet MS, *Nat Mater*, 2011, 10, 799–806. [PubMed: 21874004]
143. Truby RL and Lewis JA, *Nature*, 2016, 540, 371–378. [PubMed: 27974748]
144. Xing JF, Zheng ML and Duan XM, *Chem Soc Rev*, 2015, 44, 5031–5039. [PubMed: 25992492]
145. Bell A, Kofron M and Nistor V, *Biofabrication*, 2015, 7, 035007. [PubMed: 26335389]
146. Yucel T, Cebeci P and Kaplan DL, *Biophys J*, 2009, 97, 2044–2050. [PubMed: 19804736]
147. Colosi C, Shin SR, Manoharan V, Massa S, Costantini M, Barbetta A, Dokmeci MR, Dentini M and Khademhosseini A, *Adv Mater*, 2016, 28, 677–684. [PubMed: 26606883]
148. Fedorovich NE, De Wijn JR, Verbout AJ, Alblas J and Dhert WJ, *Tissue Eng Part A*, 2008, 14, 127–133. [PubMed: 18333811]
149. Duarte Campos DF, Blaeser A, Korsten A, Neuss S, Jakel J, Vogt M and Fischer H, *Tissue Eng Part A*, 2015, 21, 740–756. [PubMed: 25236338]
150. Billiet T, Gevaert E, De Schryver T, Cornelissen M and Dubruel P, *Biomaterials*, 2014, 35, 49–62. [PubMed: 24112804]
151. Levato R, Webb WR, Otto IA, Mensinga A, Zhang Y, van Rijen M, van Weeren R, Khan IM and Malda J, *Acta Biomater*, 2017, 61, 41–53. [PubMed: 28782725]

152. Mouser VH, Melchels FP, Visser J, Dhert WJ, Gawlitta D and Malda J, *Biofabrication*, 2016, 8, 035003. [PubMed: 27431733]
153. Brown GCJ, Lim KS, Farrugia BL, Hooper GJ and Woodfield TBF, *Macromol Biosci*, 2017, 17, 1700158.
154. Levato R, Visser J, Planell JA, Engel E, Malda J and Mateos-Timoneda MA, *Biofabrication*, 2014, 6, 035020. [PubMed: 25048797]
155. Duan B, Hockaday LA, Kang KH and Butcher JT, *J Biomed Mater Res A*, 2013, 101, 1255–1264. [PubMed: 23015540]
156. Pimentel CR, Ko SK, Caviglia C, Wolff A, Emneus J, Keller SS and Dufva M, *Acta Biomater*, 2018, 65, 174–184. [PubMed: 29102798]
157. Malana MA, Zohra R and Khan MS, *Korea-Australia Rheology Journal*, 2012, 24, 155–162.
158. Zhang W, Soman P, Meggs K, Qu X and Chen S, *Adv Funct Mater*, 2013, 23, 3226–3232.
159. Malda J, Visser J, Melchels FP, Jungst T, Hennink WE, Dhert WJ, Groll J and Hutmacher DW, *Adv Mater*, 2013, 25, 5011–5028. [PubMed: 24038336]
160. Ratner ASHBD, Schoen FJ and Lemons JE, *Biomaterials science: an introduction to materials in medicine*, 2013.
161. Zhang J. P. F. a. K. W. L. L. G., Elsevier Academic Press, 2015.
162. Martínez Ávila H, Schwarz S, Rotter N and Gatenholm P, *Bioprinting*, 2016, 1–2, 22–35.
163. Ouyang L, Highley CB, Rodell CB, Sun W and Burdick JA, *ACS Biomaterials Science & Engineering*, 2016, 2, 1743–1751. [PubMed: 33440472]
164. Gao Q, He Y, Fu JZ, Liu A and Ma L, *Biomaterials*, 2015, 61, 203–215. [PubMed: 26004235]
165. Faulkner-Jones A, Fyfe C, Cornelissen DJ, Gardner J, King J, Courtney A and Shu W, *Biofabrication*, 2015, 7, 044102. [PubMed: 26486521]
166. Keane TJ and Badylak SF, *Semin Pediatr Surg*, 2014, 23, 112–118. [PubMed: 24994524]
167. Hospodiuk M, Dey M, Sosnoski D and Ozbolat IT, *Biotechnol Adv*, 2017, 35, 217–239. [PubMed: 28057483]
168. Pati F, Jang J, Ha DH, Won Kim S, Rhie JW, Shim JH, Kim DH and Cho DW, *Nat Commun*, 2014, 5, 3935. [PubMed: 24887553]
169. Lee H, Han W, Kim H, Ha DH, Jang J, Kim BS and Cho DW, *Biomacromolecules*, 2017, 18, 1229–1237. [PubMed: 28277649]
170. Gopinathan J and Noh I, *Biomater Res*, 2018, 22, 11. [PubMed: 29636985]
171. Ashammakhi N, Ahadian S, Xu C, Montazerian H, Ko H, Nasiri R, Barros N and Khademhosseini A, *Materials Today Bio*, 2019, 1, 100008.
172. Pawar AA, Saada G, Cooperstein I, Larush L, Jackman JA, Tabaei SR, Cho NJ and Magdassi S, *Sci Adv*, 2016, 2, e1501381. [PubMed: 27051877]
173. Crapo PM, Gilbert TW and Badylak SF, *Biomaterials*, 2011, 32, 3233–3243. [PubMed: 21296410]
174. Sellaro TL, Ranade A, Faulk DM, McCabe GP, Dorko K, Badylak SF and Strom SC, *Tissue Eng Part A*, 2010, 16, 1075–1082. [PubMed: 19845461]
175. Perniconi B, Costa A, Aulino P, Teodori L, Adamo S and Coletti D, *Biomaterials*, 2011, 32, 7870–7882. [PubMed: 21802724]
176. Kelly BE, Bhattacharya I, Heidari H, Shusteff M, Spadaccini CM and Taylor HK, *Science*, 2019, 363, 1075–1079. [PubMed: 30705152]
177. Hounsfield GN, Patent No US. 3778614, 1973.
178. Heinzl J. K. a. C., Springer, 2015.
179. Bortfeld T, Burkelbach J, Boesecke R and Schlegel W, *Phys Med Biol*, 1990, 35, 1423–1434. [PubMed: 2243845]
180. Grigoryan B, Paulsen SJ, Corbett DC, Sazer DW, Fortin CL, Zaita AJ, Greenfield PT, Calafat NJ, Gounley JP, Ta AH, Johansson F, Randles A, Rosenkrantz JE, Louis-Rosenberg JD, Galie PA, Stevens KR and Miller JS, *Science*, 2019, 364, 458–464. [PubMed: 31048486]
181. Skylar-Scott MA, Mueller J, Visser CW and Lewis JA, *Nature*, 2019, 575, 330–335. [PubMed: 31723289]

182. Wu W, DeConinck A and Lewis JA, *Adv Mater*, 2011, 23, H178–183. [PubMed: 21438034]
183. Bhattacharjee T, Zehnder SM, Rowe KG, Jain S, Nixon RM, Sawyer WG and Angelini TE, *Sci Adv*, 2015, 1, e1500655. [PubMed: 26601274]
184. Hinton TJ, Jallerat Q, Palchesko RN, Park JH, Grodzicki MS, Shue HJ, Ramadan MH, Hudson AR and Feinberg AW, *Sci Adv*, 2015, 1, e1500758. [PubMed: 26601312]
185. Highley CB, Rodell CB and Burdick JA, *Adv Mater*, 2015, 27, 5075–5079. [PubMed: 26177925]
186. Loebel C, Rodell CB, Chen MH and Burdick JA, *Nat Protoc*, 2017, 12, 1521–1541. [PubMed: 28683063]
187. Highley CB, Song KH, Daly AC and Burdick JA, *Adv Sci (Weinh)*, 2019, 6, 1801076. [PubMed: 30643716]
188. Luo G, Yu Y, Yuan Y, Chen X, Liu Z and Kong T, *Adv Mater*, 2019, 31, e1904631. [PubMed: 31609497]
189. Skylar-Scott MA, Uzel SGM, Nam LL, Ahrens JH, Truby RL, Damaraju S and Lewis JA, *Sci Adv*, 2019, 5, eaaw2459. [PubMed: 31523707]
190. Tibbitts S, *Architectural Design*, 2014, 84, 116–121.
191. Khoo ZX, Teoh JEM, Liu Y, Chua CK, Yang S, An J, Leong KF and Yeong WY, *Virtual and Physical Prototyping*, 2015, 10, 103–122.
192. Zhang Z, Demir KG and Gu GX, *International Journal of Smart and Nano Materials*, 2019, 10, 205–224.
193. Miao S, Zhu W, Castro NJ, Nowicki M, Zhou X, Cui H, Fisher JP and Zhang LG, *Sci Rep*, 2016, 6, 27226. [PubMed: 27251982]
194. Bodaghi M, Damanpack AR and Liao WH, *Smart Materials and Structures*, 2016, 25, 105034.
195. Kwok T-H, Wang CCL, Deng D, Zhang Y and Chen Y, *Journal of Mechanical Design*, 2015, 137, 111413.
196. Zhang Y, Zhang F, Yan Z, Ma Q, Li X, Huang Y and Rogers JA, *Nature Reviews Materials*, 2017, 2, 17019.
197. Ge Q, Sakhaei AH, Lee H, Dunn CK, Fang NX and Dunn ML, *Sci Rep*, 2016, 6, 31110. [PubMed: 27499417]
198. Yu K, Ritchie A, Mao Y, Dunn ML and Qi HJ, *Procedia IUTAM*, 2015, 12, 193–203.
199. Momeni F, Sabzpooshan S, Valizadeh R, Morad MR, Liu X and Ni J, *Renewable Energy*, 2019, 130, 329–351.
200. Hager MD, Bode S, Weber C and Schubert US, *Progress in Polymer Science*, 2015, 49–50, 3–33.
201. Ge Q, Qi HJ and Dunn ML, *Applied Physics Letters*, 2013, 103, 131901.
202. Lan X, Liu Y, Lv H, Wang X, Leng J and Du S, *Smart Materials and Structures*, 2009, 18, 024002.
203. Wei H, Zhang Q, Yao Y, Liu L, Liu Y and Leng J, *ACS Appl Mater Interfaces*, 2017, 9, 876–883. [PubMed: 27997104]
204. Zhang Q, Zhang K and Hu G, *Sci Rep*, 2016, 6, 22431. [PubMed: 26926357]
205. Malachowski K, Breger J, Kwag HR, Wang MO, Fisher JP, Selaru FM and Gracias DH, *Angew Chem Int Ed Engl*, 2014, 53, 8045–8049. [PubMed: 24634136]
206. Azam A, Laflin KE, Jamal M, Fernandes R and Gracias DH, *Biomed Microdevices*, 2011, 13, 51–58. [PubMed: 20838901]
207. Therien-Aubin H, Wu ZL, Nie Z and Kumacheva E, *J Am Chem Soc*, 2013, 135, 4834–4839. [PubMed: 23464872]
208. Zarek M, Mansour N, Shapira S and Cohn D, *Macromol Rapid Commun*, 2017, 38, 015002.
209. Hippler M, Blasco E, Qu J, Tanaka M, Barner-Kowollik C, Wegener M and Bastmeyer M, *Nat Commun*, 2019, 10, 232. [PubMed: 30651553]
210. Zhang L, Liang H, Jacob J and Naumov P, *Nat Commun*, 2015, 6, 7429. [PubMed: 26067649]
211. Raviv D, Zhao W, McKnelly C, Papadopoulou A, Kadambi A, Shi B, Hirsch S, Dikovskiy D, Zyracki M, Olguin C, Raskar R and Tibbitts S, *Sci Rep*, 2014, 4, 7422. [PubMed: 25522053]
212. Mao Y, Ding Z, Yuan C, Ai S, Isakov M, Wu J, Wang T, Dunn ML and Qi HJ, *Sci Rep*, 2016, 6, 24761. [PubMed: 27109063]

213. Gladman AS, Matsumoto EA, Nuzzo RG, Mahadevan L and Lewis JA, *Nat Mater*, 2016, 15, 413–418. [PubMed: 26808461]
214. Mulakkal MC, Trask RS, Ting VP and Seddon AM, *Materials & Design*, 2018, 160, 108–118.
215. Zhang K, Kimball JS, Nemani RR, Running SW, Hong Y, Gourley JJ and Yu Z, *Sci Rep*, 2015, 5, 15956. [PubMed: 26514110]
216. Breger JC, Yoon C, Xiao R, Kwag HR, Wang MO, Fisher JP, Nguyen TD and Gracias DH, *ACS Appl Mater Interfaces*, 2015, 7, 3398–3405. [PubMed: 25594664]
217. Wang G, Yao L, Wang W, Ou J, Cheng C-Y and Ishii H, presented in part at the Proceedings of the 2016 CHI Conference on Human Factors in Computing Systems - CHI '16, 2016.
218. Lv C, Xia H, Shi Q, Wang G, Wang Y-S, Chen Q-D, Zhang Y-L, Liu L-Q and Sun H-B, *Advanced Materials Interfaces*, 2017, 4, 1601002.
219. Lei D, Yang Y, Liu Z, Chen S, Song B, Shen A, Yang B, Li S, Yuan Z, Qi Q, Sun L, Guo Y, Zuo H, Huang S, Yang Q, Mo X, He C, Zhu B, Jeffries EM, Qing F-L, Ye X, Zhao Q and You Z, *Materials Horizons*, 2019, 6, 394–404.
220. Yang H, Leow WR, Wang T, Wang J, Yu J, He K, Qi D, Wan C and Chen X, *Advanced Materials*, 2017, 29.
221. Liu Y, Shaw B, Dickey MD and Genzer J, *Sci Adv*, 2017, 3, e1602417. [PubMed: 28275736]
222. Kuksenok O and Balazs AC, *Materials Horizons*, 2016, 3, 53–62.
223. Mu X, Sowan N, Tumbic JA, Bowman CN, Mather PT and Qi HJ, *Soft Matter*, 2015, 11, 2673–2682. [PubMed: 25690905]
224. Wu J, Zhao Z, Kuang X, Hamel CM, Fang D and Qi HJ, *Multifunctional Materials*, 2018, 1, 015002.
225. Gupta MK, Meng F, Johnson BN, Kong YL, Tian L, Yeh YW, Masters N, Singamaneni S and McAlpine MC, *Nano Lett*, 2015, 15, 5321–5329. [PubMed: 26042472]
226. Miriyev A, Stack K and Lipson H, *Nat Commun*, 2017, 8, 596. [PubMed: 28928384]
227. Okuzaki H, Kuwabara T, Funasaka K and Saido T, *Advanced Functional Materials*, 2013, 23, 4400–4407.
228. Kim Y, Yuk H, Zhao R, Chester SA and Zhao X, *Nature*, 2018, 558, 274–279. [PubMed: 29899476]
229. Lui YS, Sow WT, Tan LP, Wu Y, Lai Y and Li H, *Acta Biomater*, 2019, 92, 19–36. [PubMed: 31071476]
230. Yang Y, Li X, Chu M, Sun H, Jin J, Yu K, Wang Q, Zhou Q and Chen Y, *Sci Adv*, 2019, 5, eaau9490. [PubMed: 30972361]
231. Kim G and Shkel YM, *Journal of Materials Research*, 2011, 19, 1164–1174.
232. Wang J, Lu T, Yang M, Sun D, Xia Y and Wang T, *Sci Adv*, 2019, 5, eaau8769. [PubMed: 30915393]

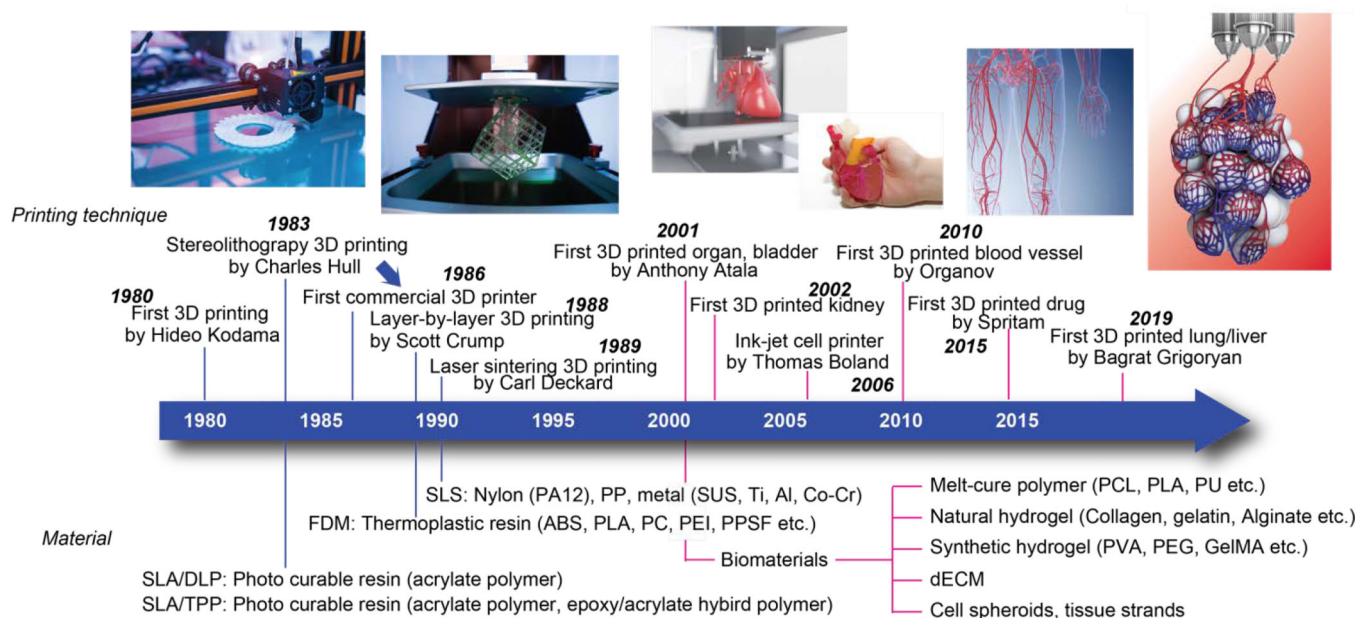


Figure 1.
Important events in the history of 3D printing.

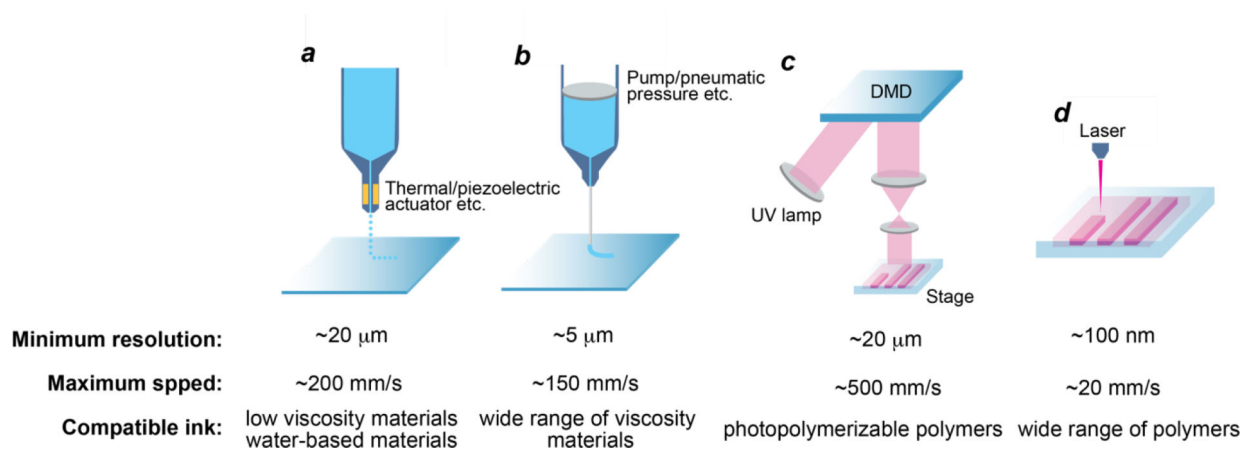


Figure 2. Schematic illustration for the primary types of 3D printing techniques. (a) inkjet-based 3D printing method. (b) extrusion-based 3D printing method. (c) dynamic optical projection stereolithography (DOPsL) 3D printing method, (d) two-photon polymerization (TPP) 3D printing method.

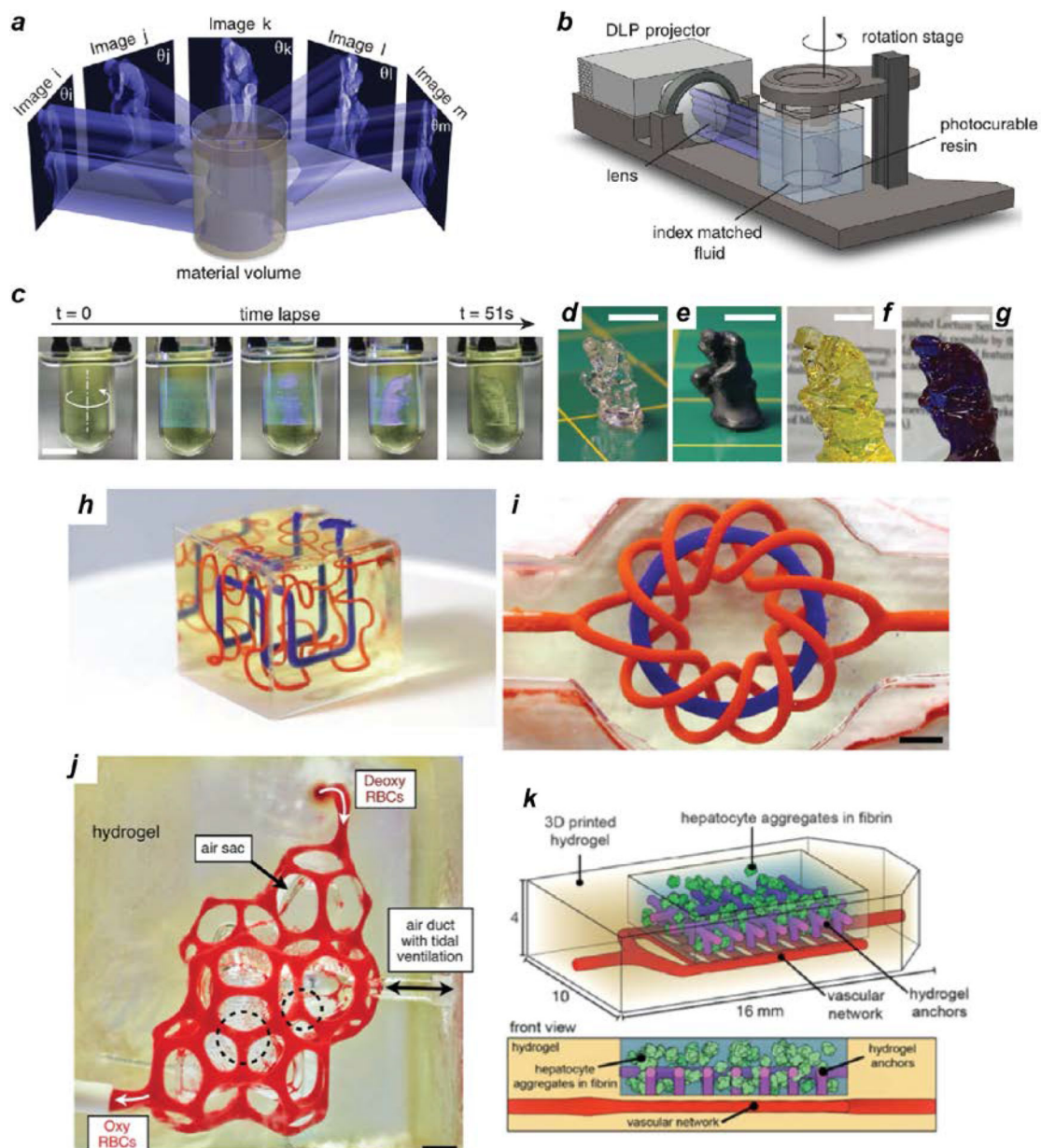


Figure 3.

(a) Underlying concept CAL volumetric fabrication. (b) Schematic of the CAL system. (c) Sequential view of the build volume during a CAL printing. (d) The object shown in (c) after rinsing away uncured resin. (e) The painted object for clarity from (d). (f) A larger version with 40-mm-tall of the same geometry. (g) Opaque version of the geometry in (f). Scale bars is 10 mm. Reproduced with permission from [176]. Copyright 2019, AAAS. (h) and (i) Entangled vascular networks with vascularized alveolar model topologies. (j) Photograph of a printed hydrogel. Scale bar is 1 mm. (k) Engraftment of functional hepatic hydrogel carriers. Reproduced with permission from [180]. Copyright 2019, AAAS.

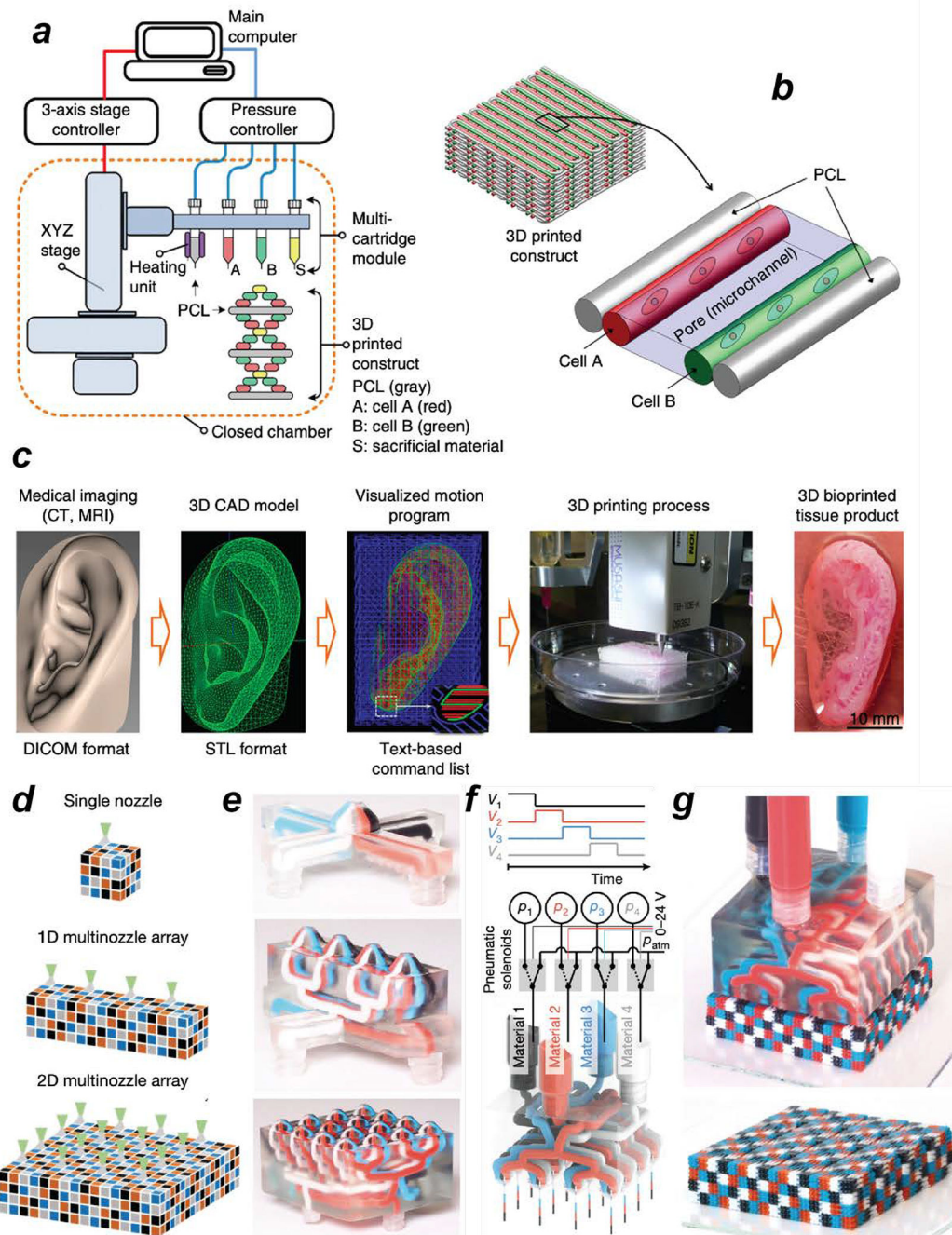


Figure 4.

(a) Schematic diagram of the ITOP system. (b) Illustration of basic patterning of 3D architecture including multiple cell-laden hydrogels and supporting PCL polymer. (c) CAD/CAM process for automated printing of 3D shape imitating target tissue or organ. Reproduced with permission from [36]. Copyright 2019, AAAS. (d) Schematic of voxelated architectures printed using a single (0D) nozzle (top) and the 1D (middle) and 2D (bottom) MM3D printheads. (e) Photographs of the corresponding 0D, 1D and 2D four-material MM3D printheads. (f) Schematic of MM3D printhead operation. (g) Voxelated matter

produced by MM3D printing using a 4×4 -nozzle, four- material, 2D printhead. Reproduced with permission from [181]. Copyright 2019, Nature Publishing Group.

Author Manuscript

Author Manuscript

Author Manuscript

Author Manuscript

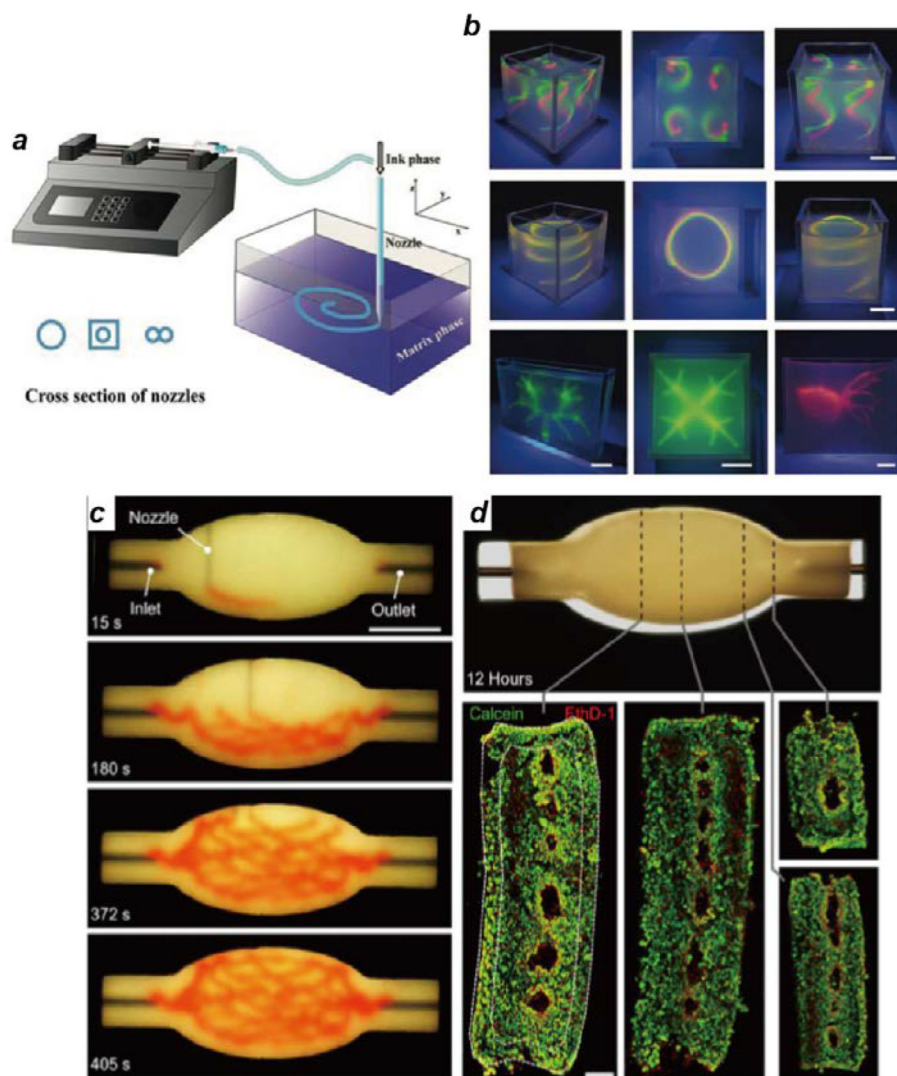


Figure 5. (a) Schematic illustration of ATPSs. (b) Photographs of double-tornado-shaped, double-spring-shaped, artery-like tree branched network, and goldfish skeleton structures. Reproduced with permission from [188]. Copyright 2019, Wiley VCH. (c) An image sequence showing the embedded 3D printing of a branched, hierarchical vascular network within a tissue matrix connected to inlet and outlet tubes. Scale bar is 10 mm. (D) Images of the perfusable tissue construct after 12 h of perfusion (top image) and fluorescent image of live/dead (green/red) cell viability (bottom images). Reproduced with permission from [189]. Copyright 2019, AAAS.

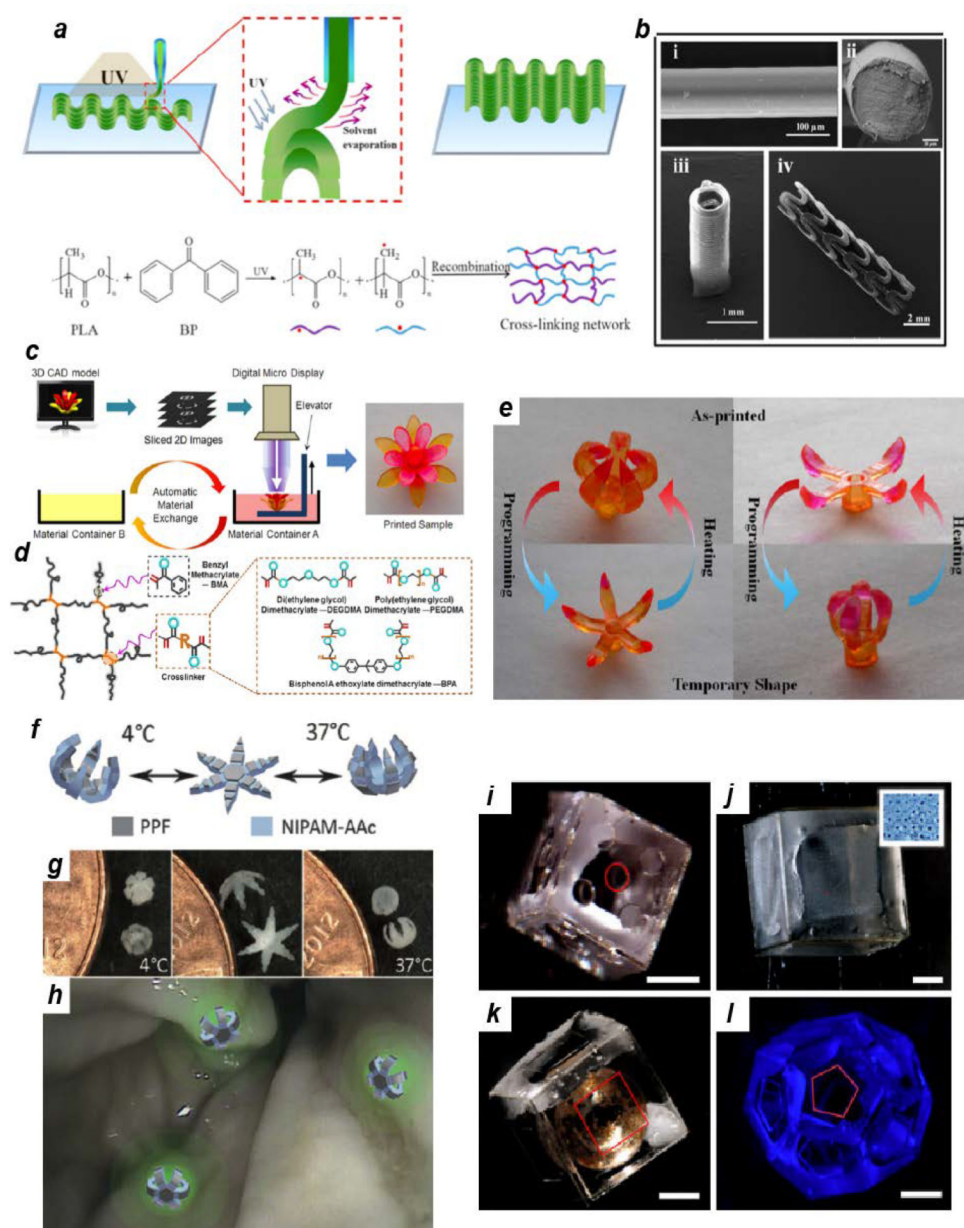


Figure 6. (a) Schematic illustration of the direct-writing printing of 4D active shape-changing architecture and the chemical structures of inks. (b) SEM images and 4D active shape-changing behavior of structures printed by c-PLA ink. Reproduced with permission from [203]. Copyright 2017, American Chemical Society. (c) and (d) Schematics of multimaterial additive manufacture system. (e) The demonstration of the transition between as printed shape and temporary shape of multimaterial grippers. Reproduced with permission from [204]. Copyright 2016, Nature Publishing Group. (f)-(h) Design and proof of principle of drug-eluting theragrippers. Reproduced with permission from [205]. Copyright 2014, Wiley VCH. (i-l) Photographs of self-folding of multiple containers and versatility in polyhedral

shape, size and precise porosity. Reproduced with permission from [206]. Copyright 2011, Springer.

Author Manuscript

Author Manuscript

Author Manuscript

Author Manuscript

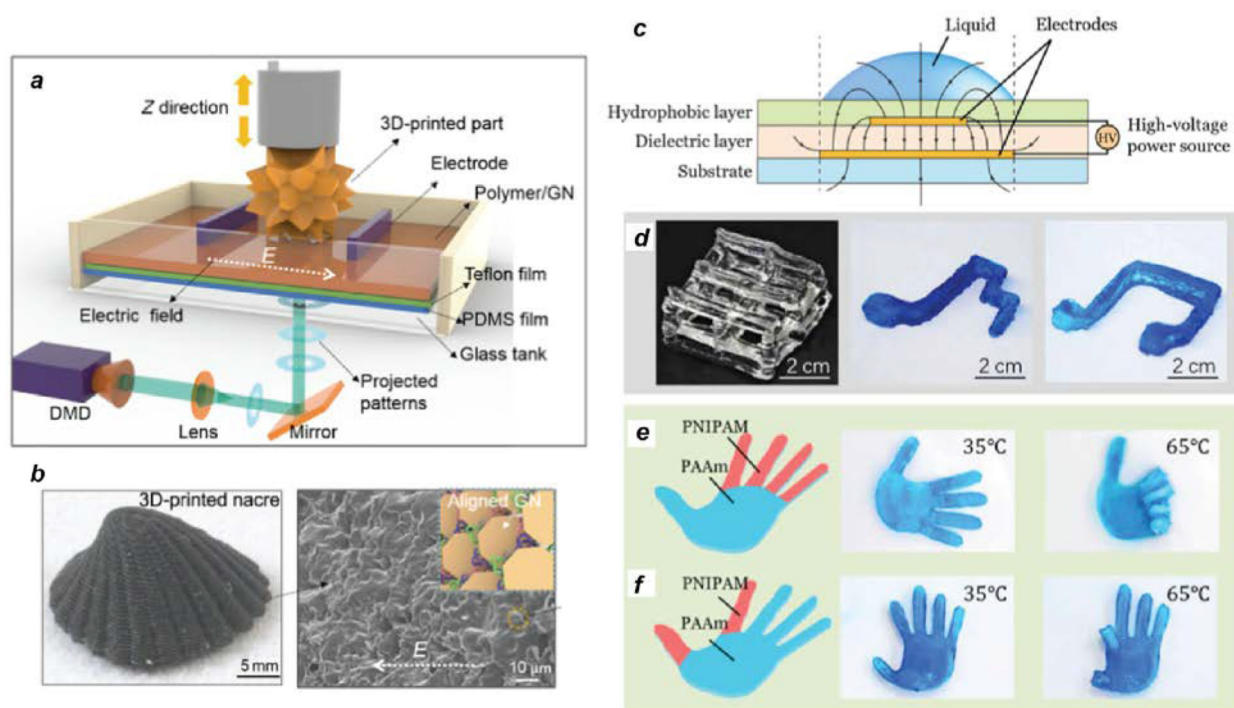


Figure 7.

(a) Schematic diagram of the electrically assisted 3D-printing platform for the construction of nacre-inspired structures, (b) 3D printed nacre with a GNs and SEM images showing surface and cross-section morphology. Reproduced with permission from [230]. Copyright 2019, AAAS. (c) Principle of PLEEC. (d) Scaffold-structured hydrogel lattice. (e) and (f) Polymerized acrylamide (PAAm) and polymerized *N*-isopropyl acrylamide (PNIPAM) hydrogel composites. Reproduced with permission from [232]. Copyright 2019, AAAS.

Table 1.

Biomaterials used for 3D printing, classified according to the type of material.

Biomaterials	Advantages	Disadvantages	Printing technique	Biomedical applications	Properties of biomedical parts	Cell viability in biomedical parts	References
				Melt-cure polymer			
PCL	High Mechanical strength, highly durable	High process temperature, low cytocompatibility, need toxic solvents	Extrusion	Liver-on-a-chip, cartilage, bone, muscle	Low protein absorption and low optical transparency for an organ-on-chip (PCL scaffolds)	HepG2 and HUVEC (<95%)	[43, 77, 88]
PLA				Heart-on-a-chip	Less absorption of hydrophobic drugs (PLA scaffolds)	Cardiomyocytes (high)	[44]
PU				Neural tissue, muscle tendon unit	High elasticity, and a stiffness same as neural tissues (PU-based muscle tendon)	C2C12 (94%) and murine NSC (<95%)	[78-81]
				Natural Hydrogel			
Alginate	High cytocompatibility, native ECM-like microenvironment	Low mechanical strength	Inkjet, pneumatic extrusion, TPP, positive displacement extrusion	Cartilage, vascular construct	High compressive modulus of 20–70 kPa (alginate constructs)	ATDC5 (>85%)	[62, 83-91]
Matrigel			Pneumatic extrusion, TPP	drug conversion on liver tissue	Capability of radiation exposure and anti-radiation drug treatment (matrigel channels)	HepG2 and M10 (high)	[89, 92]
Collagen			Inkjet, pneumatic extrusion, TPP	Liver-on-a-chip, cartilage, heterogeneous tissue construct	High mechanical stability (~25 kPa of compressive moduli) (collagen constructs)	Fibrochondrocyte (>90%)	[43, 93-95]
Gelatin			Pneumatic extrusion, TPP, positive displacement extrusion	Liver-on-a-chip	High cytocompatibility for an organ-on-chip (gelatin channels)	HepG2 and HUVEC (<95%)	[43, 80, 96-98]
Fibrinogen			Pneumatic extrusion	Skin, muscle	Deposition ability of large constructs (~100 cm ²) at a high speed (fibrin 3D scaffolds)	HaCaT keratinocytes and NIH/3T3 fibroblasts (good)	[35, 78]
Thrombin			TPP	High cell density bioink	High printing resolution and a high cell-laden density of 6×10 ⁷ cells/mL (thrombin bioinks)	High for endothelial cell	[89]
Hyaluronan			Positive displacement extrusion	Vessel-like construct	Significantly higher shear storage moduli and superior cell growth and proliferation properties (hyaluronan constructs)	NIH/3T3 (>99%)	[99]
Chitosan			Extrusion	Cartilage, bone, skin	High elastic modulus of ~6 MPa (chitosan constructs)	L929 (>70%)	[100,101]

Biomaterials	Advantages	Disadvantages	Printing technique	Biomedical applications	Properties of biomedical parts	Cell viability in biomedical parts	References
Agarose			Extrusion	Vascular network	Scaffold-free approach to construct a tubular structure (agarose templates)	Aortic smooth muscle cells (moderate)	[39, 102]
GelMA	Moderate mechanical strength, good temperature sensitivity and photocrosslink ability	Low processability	Positive displacement extrusion, DOPsL	Synthetic Hydrogel Liver-on-a-chip, vascular constructs	Superior formability and high strain moduli of 75–580 kPa (GelMA scaffolds)	3T3 and 10T1/2 (<80%)	[40,103, 98, 104]
PVA, PEG, PEGDA, PEGMA, PEGTA			Acoustic inkjet, positive displacement extrusion, SLA, DOPsL	Vascular constructs, cartilage	Good sacrificial layer ability (PVA-PEG-based hydrogels) Good elasticity tunability (PEGDA constructs)	NIH/3T3 (<80%)	[102,105–108]
Pluronic F-127, PLGA			Positive displacement extrusion	Vascular networks, cartilage, bone, muscle	Good printability, removability, and high elasticity of 2×10^4 Pa (Pluronic F-127-based inks)	HUVeC, 10T1/2, and H9cEF (<80%)	[90, 77, 109]
				Hybrid			
Gelatin-GelMA, PEG-GelMA	Good mechanical strength, high cytocompatibility		Extrusion	Muscle, vascularized bone tissues,	High compressive modulus and Young's modulus of ~5 kPa and high swelling ratio of ~35% (Gelatin-GelMA constructs)	BMSC (<90%)	[52,110, 111]
PVA-gelatin-PEG			Extrusion	Cartilage	High (~10 kPa) and low (~100 kPa) moduli (PVA-gelatin-PEG constructs)	MSC (cell activity: >75%)	[112]
Pluronic F-127-alginate			Extrusion	Muscle, Bone	High-resolution and long-term structural fidelity (Pluronic F-127-alginate constructs)	Chondrocyte and MSC (<80%)	[62,113–116]
PCL-alginate			Melt-plotting system, pneumatic extrusion	Scaffold for tissue engineering, cartilage, regenerative medicine	High Young's modulus of ~6 MPa (PCL-alginate constructs)	C20A4 (<65%)	[80, 117]
PCL-PLGA-HA-gelatin-collagen			Melt-plotting system	Scaffold for tissue engineering, cartilage, muscle	Good printability and cytocompatibility (PCL-PLGA-gelatin constructs)	Hepatocyte and MC3T3-E1 (<90%)	[118]
PCL-fibrinogen-collagen			Electrospinning	Cartilage	High Young's modulus of ~1.7 MPa and good cytocompatibility (PCL-fibrinogen-collagen constructs)	Chondrocytes (<80%)	[119]
dECM	Retain native ECM components	Low processability	Pneumatic extrusion	Muscle, bone	Natural ECM microenvironment and low Young's modulus of ~1 kPa (dECM constructs)	hASCs, L6, and hTfMSCs (<90%)	[34, 120, 168]
Other Cell spheroids, tissue strands	High cell density, no need medium or supporting material	Long process time	Extrusion	Cartilage, vascular networks, nerve grafts	High Young's modulus of ~5 MPa (tissue strands constructs)	Chondrocytes (<75%)	[39, 121–123]

Table 2.

Selected bioink properties made from natural, synthetic, and their hybrid hydrogels.

Biomaterials	Cell type	Cell density/Viability	Printing condition	Reference
Alginate 1%	NIH3T3, fibroblasts	5×10^6 /mL 90.8%	37°C, extrusion	[113, 114, 147–149]
Alginate 1–2%	Bone marrow stromal cells	2.5×10^6 /mL 95%	40°C, extrusion	
Alginate 1–4%/GelMA 4.5%	HUVECs	3×10^6 /mL 80%	RT, 1–6 mm/s, 0.08 Pa s, coaxial needle extrusion	
Collagen 0.223%	Dermal fibroblasts	1×10^6 /mL 95%	37°C, extrusion	[110, 113, 114, 147]
Collagen 15 mg mL ⁻¹ / alginate 0.1 g mL ⁻¹	Primary chondrocytes	1×10^7 /mL 90%	RT, extrusion	
PEG 10%/GelMA 5%	NIH 3T3 fibroblasts	5×10^6 /mL 85%	RT, Stereography	[110]
GelMA 5%	HUVECs, 10T1/2	40×10^6 /mL (HUVECs), 0.8×10^6 /mL (10T1/2s) 85%	RT, DLP	[40, 113, 150–154]
GelMA 10–20%	HepG2	1.5×10^6 /mL 97%	27–37°C, extrusion	
GelMA 10–20%	Articular cartilage	1.5×10^7 /mL 75–90%	37°C, extrusion	
GelMA 3–20%/ gellan gum 0–1.5%	NSCs	$10\text{--}20 \times 10^6$ /mL	RT, 475 mm/min, extrusion	
Gelatin 10–20%	Fibroblasts	5.9×10^5 /mL 91%	RT, laser direct-write	[97, 113, 114, 155, 156]
Pluronic PF127 20%/alginate 2%	C2C12	2×10^6 /mL 85%	37°C, extrusion	[62, 113, 114, 115]